12. Hunter, C.A. 2005. New IL-12-family members: IL-23 and IL-27, cytokines with divergent functions. *Nat. Rev. Immunol.* **5**:521–531.
13. McKenzie, B.S., Kastelein, R.A., and Cua, D.J. 2006. Understanding the IL-23-IL-17 immune pathway. *Trends Immunol.* **27**:17–23.
14. Aggarwal, S., Ghilardi, N., Xie, M.H., de Sauvage, F.J., and Gurney, A.L. 2003. Interleukin-23 promotes a distinct CD4 T cell activation state characterized by the production of interleukin-17. *J. Biol. Chem.* **278**:1910–1914.
15. Yen, D., et al. 2006. IL-23 is essential for T cell-mediated colitis and promotes inflammation via IL-17 and IL-6. *J. Clin. Invest.* **116**:1310–1316. doi:10.1172/JCI21404.
16. Strober, W., Fuss, I.J., and Blumberg, R.S. 2002. The immunology of mucosal models of inflammation. *Annu. Rev. Immunol.* **20**:495–549.
17. Chen, Y., et al. 2006. Anti-IL-23 therapy inhibits multiple inflammatory pathways and ameliorates autoimmune encephalomyelitis. *J. Clin. Invest.* **116**:1317–1326. doi:10.1172/JCI25308.
18. Cua, D.J., et al. 2003. Interleukin-23 rather than interleukin-12 is the critical cytokine for autoimmune inflammation of the brain. *Nature.* **421**:744–748.
19. Murphy, C.A., et al. 2003. Divergent pro- and antiinflammatory roles for IL-23 and IL-12 in joint autoimmune inflammation. *J. Exp. Med.* **198**:1951–1957.
20. Afkarian, M., et al. 2002. T-bet is a STAT1-induced regulator of IL-12R expression in naive CD4+ T cells. *Nat. Immunol.* **3**:549–557.
21. Wang, J., et al. 2006. Transcription factor T-bet regulates inflammatory arthritis through its function in dendritic cells. *J. Clin. Invest.* **116**:414–421. doi:10.1172/JCI26631.
22. Parham, C., et al. 2002. A receptor for the heterodimeric cytokine IL-23 is composed of IL-12Rbeta1 and a novel cytokine receptor subunit, IL-23R. *J. Immunol.* **168**:5699–5708.
23. Kollias, G., and Kontoyiannis, D. 2002. Role of TNF/TNFR in autoimmunity: specific TNF receptor blockade may be advantageous to anti-TNF treatments. *Cytokine Growth Factor Rev.* **13**:315–321.
24. Matsuki, T., Nakae, S., Sudo, K., Horai, R., and Iwakura, Y. 2006. Abnormal T cell activation caused by the imbalance of the IL-1/IL-1R antagonist system is responsible for the development of experimental autoimmune encephalomyelitis. *Int. Immunol.* **18**:399–407.
25. Samoilova, E.B., Horton, J.L., Hilliard, B., Liu, T.S., and Chen, Y. 1998. IL-6-deficient mice are resistant to experimental autoimmune encephalomyelitis: roles of IL-6 in the activation and differentiation of autoreactive T cells. *J. Immunol.* **161**:6480–6486.
26. Veldhoen, M., Hocking, R.J., Atkins, C.J., Locksley, R.M., and Stockinger, B. 2006. TGFbeta in the context of an inflammatory cytokine milieu supports de novo differentiation of IL-17-producing T cells. *Immunity.* **24**:179–189.
27. Shtrichman, R., and Samuel, C.E. 2001. The role of gamma interferon in antimicrobial immunity. *Curr. Opin. Microbiol.* **4**:251–259.
28. Happel, K.I., et al. 2005. Divergent roles of IL-23 and IL-12 in host defense against *Klebsiella pneumoniae*. *J. Exp. Med.* **202**:761–769.
29. Stark, M.A., et al. 2005. Phagocytosis of apoptotic neutrophils regulates granulopoiesis via IL-23 and IL-17. *Immunity.* **22**:285–294.

Role of caveolin-1 in the regulation of the vascular shear stress response

Philippe G. Frank[1,2,3] and Michael P. Lisanti[2,3]

[1]Department of Urology and [2]Departments of Molecular Pharmacology and Medicine and the Albert Einstein Diabetes Research and Training Center (DRTC), Albert Einstein College of Medicine, New York, New York, USA.
[3]Department of Cancer Biology, Kimmel Cancer Center, Thomas Jefferson University, Philadelphia, Pennsylvania, USA.

In blood vessels, endothelia are submitted to constant shear effects and are, under normal conditions, capable of responding to any variation in hemodynamic forces. Caveolae — 50- to 100-nm plasma membrane invaginations present at the surface of terminally differentiated cells and particularly enriched in ECs — are composed of a high sphingolipid and cholesterol content and the protein caveolin-1 (Cav-1). Previous studies have suggested that caveolae and endothelial Cav-1 may regulate the vascular response to altered shear stress. In this issue of the *JCI*, Yu et al. have examined the role of Cav-1/caveolae in the regulation of flow-induced alterations (i.e., mechanotransduction) in vessels from wild-type mice, Cav-1–deficient mice, and Cav-1–deficient mice re-expressing Cav-1 only in ECs. Their data suggest that caveolae/Cav-1 may act as sensors of altered shear stress and that they also organize the signaling response in stimulated ECs (see the related article beginning on page 1284).

Shear stress: an important regulator of endothelial cell function

In the vasculature, blood vessels must respond rapidly to any external stimuli and especially to any physical change related to modifications in shear stress, which is a function of the blood viscosity and the velocity gradient at the arterial wall. In this context, blood vessels need to adapt and adjust their luminal diameters and their physical properties. ECs are the primary targets of these changes, as they are the first cell type exposed to these forces. One of the earliest findings that suggested an important role for ECs in this process was the observation of the ability of ECs to reorient and change shape during exposure to shear stress conditions. When submitted to steady laminar shear stress, ECs reorient in the direction of the flow and become remarkably elongated. These observations were made both in vitro (1) and in vivo (2, 3). These findings have suggested that ECs can respond and adapt to changes in blood flow. In fact, ECs act as sensors to transduce hydrodymanic forces. Not only does the morphology of ECs change, but other important signaling pathways have been shown to be regulated in response to altered shear stress. Several studies have shown that under laminar shear stress, the rate of EC proliferation is reduced compared with static conditions (4, 5). Oscillating and/or disturbed conditions have major effects on the pathology of the vasculature. In this regard, atherosclerotic lesions have been shown to develop primarily at sites of disturbed or altered blood flow, i.e., at bifurcations, branch ostia, and curved regions (6). Under oscillating and/or disturbed conditions, EC proliferation is increased compared with cells submitted to laminar shear stress and may allow ECs to repair injuries (7, 8). Other important regulatory pathways have now been shown to be activated under shear stress conditions (9–11). These pathways include those involved in changes in endothelial apoptotic, migratory, and permeability prop-

Nonstandard abbreviations used: Cav-1, caveolin-1.

Conflict of interest: The authors have declared that no conflict of interest exists.

Citation for this article: *J. Clin. Invest.* **116**:1222–1225 (2006). doi:10.1172/JCI28509.

IL-17 Plays an Important Role in the Development of Experimental Autoimmune Encephalomyelitis[1]

Yutaka Komiyama, Susumu Nakae,[2] Taizo Matsuki,[3] Aya Nambu, Harumichi Ishigame, Shigeru Kakuta, Katsuko Sudo,[4] and Yoichiro Iwakura[5]

IL-17 is a proinflammatory cytokine that activates T cells and other immune cells to produce a variety of cytokines, chemokines, and cell adhesion molecules. This cytokine is augmented in the sera and/or tissues of patients with contact dermatitis, asthma, and rheumatoid arthritis. We previously demonstrated that IL-17 is involved in the development of autoimmune arthritis and contact, delayed, and airway hypersensitivity in mice. As the expression of IL-17 is also augmented in multiple sclerosis, we examined the involvement of this cytokine in these diseases using IL-17$^{-/-}$ murine disease models. We found that the development of experimental autoimmune encephalomyelitis (EAE), the rodent model of multiple sclerosis, was significantly suppressed in IL-17$^{-/-}$ mice; these animals exhibited delayed onset, reduced maximum severity scores, ameliorated histological changes, and early recovery. T cell sensitization against myelin oligodendrocyte glycoprotein was reduced in IL-17$^{-/-}$ mice upon sensitization. The major producer of IL-17 upon treatment with myelin digodendrocyte glycopritein was CD4$^+$ T cells rather than CD8$^+$ T cells, and adoptive transfer of IL-17$^{-/-}$ CD4$^+$ T cells inefficiently induced EAE in recipient mice. Notably, IL-17-producing T cells were increased in IFN-$\gamma^{-/-}$ cells, while IFN-γ-producing cells were increased in IL-17$^{-/-}$ cells, suggesting that IL-17 and IFN-γ mutually regulate IFN-γ and IL-17 production. These observations indicate that IL-17 rather than IFN-γ plays a crucial role in the development of EAE. *The Journal of Immunology,* **2006, 177: 566–573.**

The cytokine IL-17 can activate the expression of a variety of proinflammatory cytokines, chemokines, and cell adhesion molecules throughout a wide range of cell types, including macrophages, dendritic cells, T cells, synovial cells, and endothelial cells (1). Augmented expression of this cytokine is observed in patients with various diseases, such as rheumatoid arthritis (RA)[6] (2), systemic lupus erythematosus (3), Behcet's disease (4), allograft rejection (5), nephritic syndrome (6), asthma (7), and multiple sclerosis (MS) (8), suggesting the involvement of IL-17 in the development of these diseases. We have also demonstrated the contribution of IL-17 to the development of allergic and autoimmune diseases in mice, including contact dermatitis, airway inflammation, and arthritis (9–11). IL-17 also plays an important role in the host defense mechanisms protecting against *Klebsiella pneumoniae* infection (12). However, the role of IL-17 has only been elucidated in a few diseases and the role of this cytokine in the pathogenesis of most diseases remains largely unknown.

IL-17 is produced by a variety of cell types. A subset of Th0 and Th1 cell clones, but not Th2 cell clones, that were established from the synovial tissues of RA patients produced IL-17 (13). A number of Th0, Th1, and Th2 clones established from patients with allergic contact dermatitis also produce this cytokine (14). IL-17 is also produced by TNF-α- and/or GM-CSF-producing CD4$^+$ T cells isolated from the synovial fluid of patients with Lyme arthritis, which exhibit neither a Th1 nor a Th2 phenotype (15). Eosinophils from patients with asthma are also reported to produce this cytokine (16). Both lung neutrophils from mice treated with LPS and CD8$^+$ T cells derived from mice infected with *Klebsiella pneumoniae* are producers of IL-17 (17, 18). Thus, the producer cells of IL-17 differ in a manner dependent on the disease.

Experimental autoimmune encephalomyelitis (EAE), a rodent model of human MS, is induced by immunization of mice with encephalitogenic myelin Ags in the presence of adjuvants. EAE pathogenesis is characterized by inflammation of the CNS associated with demyelination and the infiltration of inflammatory cells including neutrophils and encephalitogenic myelin Ag-specific CD4$^+$ T cells. In MS patients, IL-17 mRNA and protein are increased in both brain lesions and mononuclear cells isolated from blood and cerebrospinal fluids (8, 19). IL-17 is also increased in lymphocytes derived from mice with EAE (20). Although these observations suggest that IL-17 may contribute to the development of MS and EAE, the precise role of this cytokine in the pathogenesis of these diseases is still poorly understood.

In this report, we have investigated the role of IL-17 in the development of the EAE using IL-17$^{-/-}$ mice. We demonstrated that the development of EAE was markedly suppressed in IL-17$^{-/-}$ mice. We also determined that IL-17 was important for the optimal activation of myelin oligodendrocyte glycoprotein

Center for Experimental Medicine, Institute of Medical Science, University of Tokyo, Tokyo, Japan

Received for publication August 30, 2005. Accepted for publication April 7, 2006.

The costs of publication of this article were defrayed in part by the payment of page charges. This article must therefore be hereby marked *advertisement* in accordance with 18 U.S.C. Section 1734 solely to indicate this fact.

[1] This work was supported by grants from the Ministry of Education, Culture, Sports, and Science of Japan, and the Ministry of Health and Welfare of Japan.

[2] Current address: Department of Pathology, Stanford University School of Medicine, 269 Campus Drive, Center for Clinical Sciences Research 3255, Stanford, CA 94305-5176.

[3] Current address: ERATO Yanagisawa Orphan Receptor Project, Japan Science and Technology Agency, Koto-Ku, Japan.

[4] Current address: Animal Research Center, Tokyo Medical University, Sinjyuku-ku, Tokyo 160-8402, Japan.

[5] Address correspondence and reprint requests to Dr. Yoichiro Iwakura, Center for Experimental Medicine, Institute of Medical Science, University of Tokyo, 4-6-1 Shirokanedai, Minato-ku, Tokyo 108-8639, Japan. E-mail address: iwakura@ims.u-tokyo.ac.jp

[6] Abbreviations used in this paper: RA, rheumatoid arthritis; MS, multiple sclerosis; EAE, experimental autoimmune encephalomyelitis; MOG, myelin oligodendrocyte glycoprotein; PTx, pertussis toxin; LN, lymph node; rm, recombinant human; GVHR, graft-vs-host reaction; CIA, collagen-induced arthritis; IDDM, insulin-dependent diabetes mellitus.

0022-1767/06/$02.00

(MOG)-specific T cells. In this model, $CD4^+$ T cells were the major producers of IL-17 in this system.

Materials and Methods

Mice

IL-$17^{-/-}$ mice (9), generated as described previously, were backcrossed to the C57BL/6J strain (six or nine generations). C57BL/6J and IFN-$\gamma^{-/-}$ mice, both on the C57BL/6J background were purchased from Japan SLC and from The Jackson Laboratory, respectively. Mice were kept under pathogen-free conditions in an environmentally controlled clean room at the Center for Experimental Medicine, Institute of Medical Science, University of Tokyo. All experiments were conducted according to the institutional ethical guidelines for animal experimentation and the safety guidelines for genetic manipulation experiments.

Induction of EAE

Active EAE. The MOG_{35-55} peptide (MEVGWYRSPFSRVVHLYRNGK) was synthesized and purified by HPLC at our institute (Dr. S. Imajoh-Ohmi, Division of Molecular Biology, Institute of Medical Science, University of Tokyo). Mice (8–13 wk of age) were immunized s.c. in one flank on day 0 and in the other on day 7 with 300 μg of MOG_{35-55} peptide emulsified in CFA (1:1), which consisted of IFA with 5 mg/ml *Mycobacterium tuberculosis* H37RA (Difco Laboratories). Pertussis toxin (PTx; Alexis) (200 ng) was injected i.v. on days 0 and 2. Following the first immunization, the severity of EAE was monitored and graded on a scale of 0–5: 0, no disease; 1, limp tail; 2, hind limb weakness; 3, hind limb paralysis; 4, hind and fore limb paralysis; 5, moribundity and death.

Passive EAE. Mice were immunized s.c. with MOG/CFA. Ten days after the immunization, the spleen and inguinal and axillary lymph nodes (LNs) were collected and a single-cell suspension was prepared. Pooled lymphocytes (4×10^6 cells/ml) were cultured in the presence of 50 μg/ml MOG_{35-55} peptide in RPMI 1640 medium containing 50 μM 2-ME, 50 μg/ml streptomycin, 50 μg/ml penicillin, and 10% heat-inactivated FBS (Sigma-Aldrich) for 4 days. After harvesting, $CD4^+$ T cells were purified by positive selection using an AutoMACS system (Miltenyi Biotec). Isolated $CD4^+$ T cells (4×10^6) were then transferred i.v. into naive C57BL/6J mice.

Histology

On day 42 after the first immunization with MOG/CFA and PTx, spines were harvested and fixed with neutral 10% formalin. Spinal cords were then extracted and embedded in paraffin. Sections (5 μm) were stained with H&E.

MOG-specific LN cell proliferation assay

Mice were immunized s.c. with MOG/CFA. Ten days after immunization, the inguinal and axillary LNs were collected and a single-cell suspension was prepared. LN cells ($1–4 \times 10^5$ cells/well) were cultured for 72 h in the absence or presence of various concentrations of MOG_{35-55} peptide as described above. Isolated cells were then pulsed for 6 h with [^{3}H]thymidine (0.25 μCi/ml; Amersham Biosciences), and harvested using a Micro 96 cell harvester (Skatron). Levels of radioactivity were measured using a Micro β system (Pharmacia Biotech).

Measurement of cytokine levels by ELISA

To detect IFN-γ and IL-4 in culture supernatants, we used mouse IFN-γ OptEIA kit (BD Pharmingen) and IL-4 ELISA kit (Endogen). Detection of IL-17 by ELISA was performed as described previously (9).

Flow cytometry

To examine LN cell population, inguinal and axillary LN cells were harvested 10 days after immunization with MOG/CFA. After incubation of cells on ice with anti-mouse CD16/CD32 mAb (2.4G2) in a staining buffer (Hank's buffer containing 2% FCS and 0.1% sodium azide) on ice for 15 min, cells were incubated on ice for 45 min with either FITC-anti-mouse CD45RB (C363.16A) or FITC anti-mouse CD62L (MEL-14) in the presence of PE anti-mouse CD44 (Pgp-1) and allophycocyanin anti-mouse CD4 (RM4-5). 7-Aminoactinomycin D (Sigma-Aldrich)-negative, $CD4^+$ cells were examined by a FACSCalibur (BD Biosciences) using CellQuest software (BD Biosciences). To detect IL-17 production in lymphocytes (T cells and B cells), LN cells were harvested 10 days after immunization with MOG/CFA. Isolated cells were cultured in the presence or absence of 50 μg/ml MOG_{35-55} peptide for 72 h as described above. To examine IL-17 production by $Gr\text{-}1^+$ neutrophils, we prepared a single-cell suspension from the spleens of EAE-affected wild-type mice (day 42). LN cells (72 h after cultivation) and spleen cells were stimulated for 6 h with 20 ng/ml PMA (Sigma-Aldrich), 1 μM ionomycin (Sigma-Aldrich), and 2 μM monensin (Sigma-Aldrich) for 6 h. After harvesting, cells were incubated on ice with anti-mouse CD16/CD32 mAb (2.4G2) in a staining buffer on ice for 15 min. Cell samples were then incubated on ice for 45 min with either FITC-anti-mouse B220 (RA3-6B2), FITC anti-mouse Gr-1 (RB6-8C5), or FITC anti-mouse CD3ε (145-2C11), allophycocyanin anti-mouse CD4 (RM4-5 or GK1.5), or allophycocyanin anti-mouse CD8α (53-6.7) Abs. After washing, the cells were fixed in a fixation buffer (2% paraformaldehyde in PBS) at room temperature for 10 min. Samples were then permeabilized with permeabilization buffer (staining buffer containing 0.1% saponin) and incubated for 30 min with PE-conjugated anti-mouse IL-17 mAb (TC11-18H10) or isotype-matched control rat IgG1 (R3-34) at 4°C. The cells were analyzed on a FACSCalibur flow cytometer as described above. All mAbs were purchased from BD Pharmingen.

$CD4^+$ T cell cultures

$CD4^+$ T cells (< 95%) from wild-type mouse spleen were purified by MACS system as described elsewhere (9), then stimulated with 1.0 μg/ml plate-coated anti-CD3 mAb (145-2C11; BD Pharmingen) in the presence or absence of various concentration of recombinant mouse IFN-γ

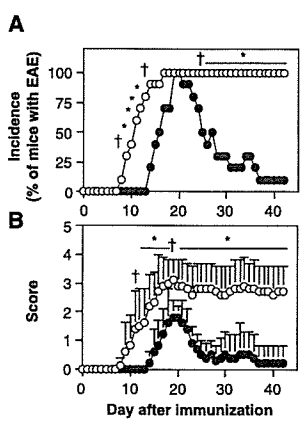

FIGURE 1. Development of EAE was reduced in IL-$17^{-/-}$ mice. EAE was induced in mice by immunization with MOG/CFA coinjected with PTx. *A*, Incidence of EAE. *B*, Clinical scores of diseased mice. ○, Wild-type mice ($n = 10$); ●, IL-$17^{-/-}$ mice ($n = 10$). Data are the averages ± SD for each group. †, $p < 0.05$ and *, $p < 0.001$ vs IL-$17^{-/-}$ mice by Mann-Whitney's U test (*A*) and by χ^2 test (*B*), respectively.

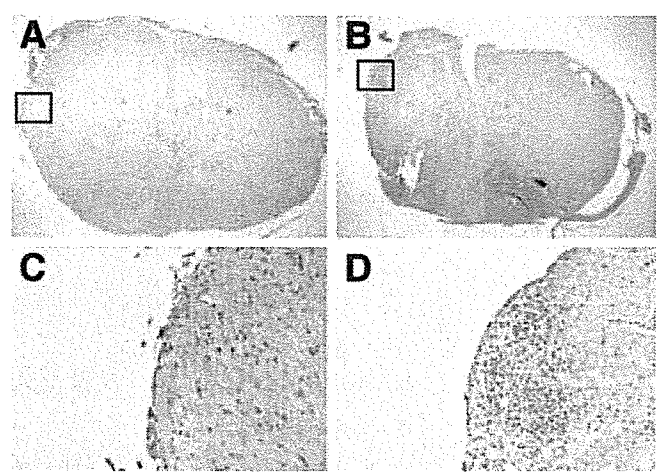

FIGURE 2. Local inflammation of the CNS was suppressed in IL-$17^{-/-}$ mice during EAE. On day 42 after MOG/CFA and PTx immunization, spinal cords were removed. The tissue sections were stained with H&E. The sections at the lumbar level are shown. *A* and *C*, IL-$17^{-/-}$ mice. *B* and *D*, Wild-type mice. *A* and *B*, ×40. *C* and *D*, ×200.

(rmIFN-γ; PeproTech), rmIL-12 (R&D Systems), rmIL-17 (R&D Systems), and rmIL-23 (R&D Systems) for 48 h. Then, culture supernatants were collected and IFN-γ or IL-17 levels in the supernatants were determined by ELISA as described above.

Measurement of MOG-specific serum Ab levels by ELISA

A 96-well flat-bottom plate (Falcon 3912 Micro test III Flexible Assay Plates; BD Biosciences) was coated with 10 μg/ml MOG_{35-55} peptides at 4°C overnight. After washing the wells with 0.05% Tween 20 in PBS, the wells were blocked with PBS containing 1% skim milk, 5 mM EDTA, 0.02% NaN3 for 1 h at room temperature. After washing, diluted serum samples were added and incubated for 2 h at room temperature. Then, after washing the wells, alkaline phosphatase-conjugated goat anti-mouse Igs (IgG, IgG1, IgG2a, IgG2b, IgG3, IgM; Zymed Laboratories) were added and incubated for 1 h at room temperature. Alkaline phosphatase activity was measured using Substrate Phosphatase SIGMA104 (Sigma-Aldrich). The anti-MOG Ab titer was shown as OD_{415} values.

Statistics

The Student *t* test, the Mann-Whitney's *U* test, or the χ^2 test was used for the statistical evaluation of the results.

Results

Development EAE was suppressed in IL-17$^{-/-}$ mice

To investigate the role of IL-17 in the pathogenesis of EAE, we examined the effect of IL-17-deficiency on the development of EAE using IL-17$^{-/-}$ mice. To induce EAE, mice were treated with MOG_{35-55} peptide emulsified in CFA and injected with PTx. The initial signs of EAE were observed 10 days after the first immunization of wild-type mice (Fig. 1). In contrast, the onset of EAE was significantly delayed in IL-17$^{-/-}$ mice until day 15 (Fig. 1). Twenty days after the first immunization, however, IL-17$^{-/-}$ mice exhibited a similar incidence of EAE as that seen in wild-type mice (Fig. 1*A*), although the severity of disease in IL-17$^{-/-}$ mice was milder than that in wild-type mice (Fig. 1*B*). After day 20 from the immunization, the severe signs of disease continued in wild-type mice, while early amelioration was observed in IL-17$^{-/-}$ mice (Fig. 1*A*). Consistent with these observations, a massive infiltration of mononuclear cells was observed within the spinal cords of wild-type mice 42 days after the first immunization (Fig. 2, *B* and *D*). In contrast, the cellular infiltration was significantly reduced in IL-17$^{-/-}$ mice (Fig. 2, *A* and *C*).

PTx is widely used to enhance the development of T cell-mediated organ-specific autoimmune diseases, including EAE. TNF-α$^{-/-}$ mice develop EAE normally when high doses of PTx are injected, while in the presence of low doses of PTx, mutant mice exhibit significantly reduced development of EAE symptoms (21). Thus, PTx may sometimes mask or compensate for the pathological functions of some proinflammatory mediators, such as TNF-α, in the pathogenesis of EAE. Therefore, to more clearly observe the effect of IL-17 deficiency, we next induced EAE in IL-17$^{-/-}$ mice in the absence of PTx treatment. Under these conditions, disease onset in IL-17$^{-/-}$ mice delayed compared with wild-type mice similarly to that seen in the presence of PTx (Fig. 3). Interestingly, in the absence of PTx, the disease also gradually ameliorated in wild-type mice after 22 days of induction, as seen for IL-17$^{-/-}$ mice, although the maximal severity score of the wild-type mice remained significantly higher (Fig. 3). These results demonstrate that IL-17 contributes to the development of EAE.

MOG- specific T cell sensitization was impaired in IL-17$^{-/-}$ mice

We previously showed that IL-17 plays an important role in Ag-specific T cell activation during the development of multiple allergic and autoimmune diseases (9–11). To compare our previous

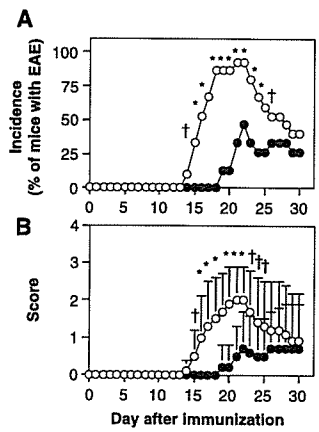

FIGURE 3. Development of EAE was reduced in IL-17$^{-/-}$ mice. Mice were induced EAE by immunization with MOG/CFA, but without PTx. *A*, Incidence of EAE. *B*, Clinical score of diseased mice. ○, Wild-type mice (n = 15), and ●, IL-17$^{-/-}$ mice (n = 15). Data are shown as an average + SD in each group. †, $p < 0.05$ and *, $p < 0.001$ vs IL-17$^{-/-}$ mice by Mann-Whitney's *U* test (*A*) and by χ^2 test (*B*).

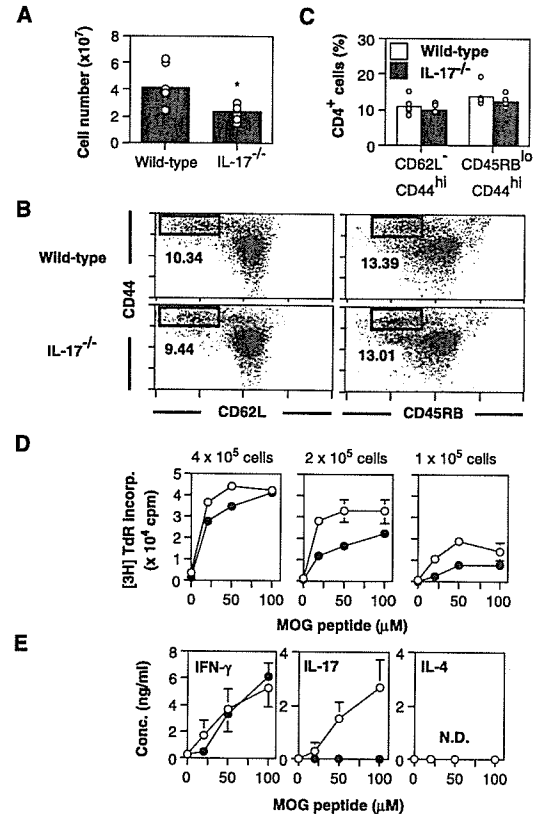

FIGURE 4. MOG-specific lymphocyte activation was impaired in IL-17$^{-/-}$ mice. Mice were immunized once with MOG/CFA in the absence of PTx, and 10 days after immunization, the inguinal and axillary LNs were collected and pooled. *A*, Total LN cell number. *B* and *C*, Percentage of $CD62L^{-}CD44^{high}$ or $CD45RB^{low}CD44^{high}$ $CD4^{+}$ T cells in LNs. In *A* and *C*, each circle represents a value from an individual mouse, and the column represents the average for each group. Representative FACS results are shown in *B*. *, $p < 0.05$ and vs the corresponding values for wild-type mice. *D*, Isolated LN cells were cultured in the absence or presence of MOG peptide for 72 h, and MOG-specific LN cell proliferation as measured by [^{3}H]thymidine incorporation (*D*) and IFN-γ, IL-17, and IL-4 levels in the culture supernatants (2×10^5 cells) (*E*) are shown. ○, Wild-type mice, and ●, IL-17$^{-/-}$ mice. Averages ± SD of triplicate wells are shown. All results are representative at least in three experiments. *D*, Data are averages ± SD from three independent experiments. N.D., Not detected.

results to the models in the current study, we next assessed the role of IL-17 in the activation of MOG-specific T cells during the development of EAE. Ten days after immunization with MOG/CFA alone (without PTx), hypertrophy of inguinal and axillary lymph nodes was observed. Although the total number of pooled inguinal and axillary LN cells was significantly decreased in IL-$17^{-/-}$ mice in comparison with wild-type mice (Fig. 4*A*), the content of memory $CD4^+$ T cells ($CD62L^-CD44^{high}$ or $CD45RB^{low}CD44^{high}$) was comparable (Fig. 4, *B* and *C*). Then, the draining LN cells were cultured in the presence or absence of MOG peptide. When a large excess of LN cells (4×10^5 cells) was present in a well, the observed MOG-specific LN cell proliferative responses in IL-$17^{-/-}$ mice were similar to those seen in wild-type LN cells (Fig. 4*D*). In the presence of an optimal number of LN cells (2×10^5 and 1×10^5 cells), the proliferative responses of cells derived from IL-$17^{-/-}$ mice were markedly decreased compared with those in wild-type mice despite similar number of memory T cells was contained in wild-type and IL-$17^{-/-}$ mouse culture (Fig. 4*D*). IL-17 was detected in the supernatants of wild-type LN cell cultures (2×10^5 cells), and its levels increased in a manner dependent on the dose of MOG peptide. IL-17 was undetectable in IL-$17^{-/-}$ LN cell cultures (2×10^5 cells) (Fig. 4*D*). The MOG-specific proliferative responses of LN T cells were reduced in IL-$17^{-/-}$ mice (Fig. 4D). Nevertheless, IFN-γ production in the LN cell culture supernatants was similar in wild-type and IL-$17^{-/-}$ mice (Fig. 4*E*). IL-4 levels in the LN cell culture supernatants from both wild-type and IL-$17^{-/-}$ mice were below the limit of detection (Fig. 4*E*). These results suggest that the delayed onset of the EAE response in IL-$17^{-/-}$ mice is caused by insufficient T cell sensitization against the MOG peptide.

$CD4^+$ T cells produced IL-17 in LN cells during EAE

Different subsets of $CD4^+$ Th cells and eosinophils are known to produce IL-17 in patients with dermatitis, RA, Lyme arthritis, and asthma (13–16). Neutrophils and $CD8^+$ T cells can also produce IL-17 during certain infectious diseases in mice (17, 18). These observations suggest that the IL-17 producer cells may differ from those known to produce this cytokine in other diseases. Thus, we next analyzed the IL-17 producer cells in the LNs of wild-type mice following MOG immunization. Ten days after immunization, inguinal and axillary LNs were collected and LN cells were cultured in the presence of MOG peptide for 72 h. After MOG stimulation, IL-17 production was detected in $CD3^+$ T cells, but not in granulocytes or B cells (Fig. 5*A*). Within the T cell population, IL-17 was predominantly produced in $CD4^+$ T cells, but at low levels in $CD8^+$ T cells (Fig. 5*B*). Thus, $CD4^+$ T cells, rather than $CD8^+$ T cells, were the major producer of IL-17 within LNs during the development of EAE.

The efficiency of EAE induction of IL-$17^{-/-}$ CD4 T cells was low in comparison with wild-type T cells

To examine the effect of IL-17 deficiency on T cell sensitization against the MOG peptide, we adoptively transferred $CD4^+$ T cells into recipient mice of the same genetic background. Lymphocytes from MOG/CFA-immunized wild-type or IL-$17^{-/-}$ mice were stimulated with MOG peptide for 4 days in vitro, and $CD4^+$ T cells were then purified and transferred into naive wild-type mice. The development of EAE in mice that received IL-$17^{-/-}$ $CD4^+$ T cells was markedly reduced in comparison to those animals receiving wild-type $CD4^+$ T cells (Fig. 6). These observations indicate that MOG-specific T cells from IL-$17^{-/-}$ mice cannot efficiently induce EAE in recipient mice.

IL-17 production was enhanced in IFN-$\gamma^{-/-}$ mice

MS and EAE are typically classified as Th1 cell-mediated autoimmune diseases. It has been shown, however, that the development of EAE is exacerbated in IFN-$\gamma^{-/-}$ and/or IFN-$\gamma R^{-/-}$ mice (22–25), indicating that IFN-γ serves a protective role in the disease pathogenesis. Therefore, we next examined whether IFN-γ-deficiency influences IL-17 production by $CD4^+$ T cells during EAE development. Consistent with previous reports, the LN (inguinal and axillary) cell number of IFN-$\gamma^{-/-}$ mice was significantly increased compared with that of wild-type mice 10 days after MOG/CFA immunization (Fig. 7*A*). When LN cells from MOG-immunized mice were cultured in the presence of MOG peptides, proliferating cells were predominantly observed in a region indicated as "R2", while nonproliferating cells were observed in a region indicated as "R1" (Fig. 7*B*), as determined by CFSE labeling (data not shown). Thus, to detect MOG-reactive, IL-17-producing T cells in LN cells, cells were selectively gated to the R2 region. The percentage of IL-17-producing $CD4^+$ T cells in the draining LN cells of IFN-$\gamma^{-/-}$ mice was greatly increased in comparison to that in wild-type mouse T cells, irrespective of MOG restimulation (Fig. 7, *C* and *D*). A large proportion of $CD8^+$ T cells, as well as $CD4^+$ T cells from IFN-$\gamma^{-/-}$ mice immunized with MOG/CFA, produced IL-17, although only a small proportion of $CD8^+$ cells from wild-type mice produced IL-17 (Fig. 7, *C* and *D*).

Next, we assessed the effect of IL-17 on IFN-γ production during MOG immunization. As shown in Fig. 4, *D* and *E*, although MOG-specific T cell proliferation was impaired in IL-$17^{-/-}$ mice, IFN-γ levels in culture supernatants were normally observed. These observations suggested that the IFN-γ-producing cell population is increased in IL-$17^{-/-}$ mice. In support of this, the percentage of IFN-γ-producing $CD4^+$ T cells in the draining LN cells

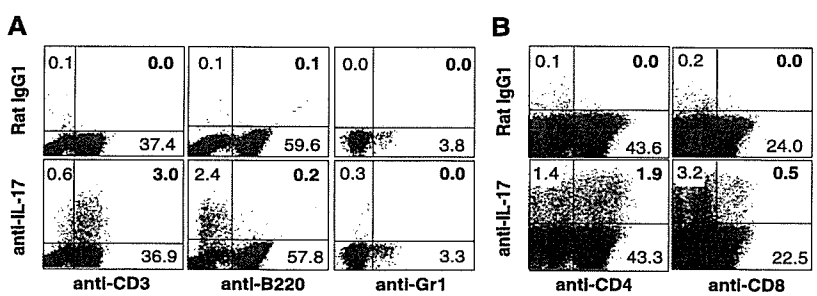

FIGURE 5. IL-17 was primarily produced by $CD4^+$ LN T cells during the development of EAE. To detect IL-17-producing cells in the lymphocyte or granulocyte populations, LN cells from mice immunized with MOG/CFA were cultured in the presence of 50 μg/ml MOG peptide for 72 h, followed by stimulation with PMA + ionomycin in the presence of monensin; then IL-17-producing cells were detected by FACS. Gr-1^+ cells were stained using spleen cells from mice with EAE. *A*, The IL-17^+ populations in $CD3^+$ or $B220^+$ cell populations within the LN cells, or the Gr-1^+ cells of the spleen. *B*, IL-17 production by $CD3^+CD4^+$ or $CD3^+CD8^+$ T cells.

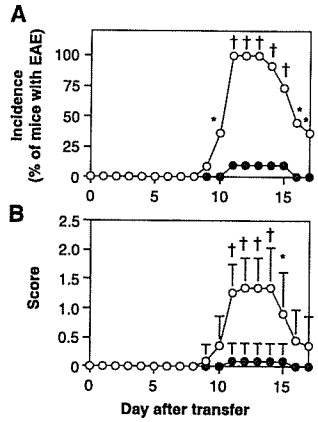

FIGURE 6. $CD4^+$ T cells were responsible for the induction of EAE. Mice were immunized once with MOG/CFA alone. At 10 days postimmunization, the spleen and the inguinal and axillary LNs were collected and pooled. The pooled cells were cultured in the presence of MOG peptide for 72 h, and then $CD4^+$ T cells were purified and transferred into naive, wild-type mice. *A*, The incidence of EAE. *B*, The clinical scores of the diseased mice. ○, Mice that received wild-type $CD4^+$ T cells ($n = 11$), and, ●, mice that received IL-$17^{-/-}$ $CD4^+$ T cells ($n = 10$). In *B*, data are shown as the averages ± SD for each group. †, $p < 0.05$ and *, $p < 0.001$ vs IL-$17^{-/-}$ mice by the Mann-Whitney's *U* test (*A*) and by the χ^2 test (*B*), respectively.

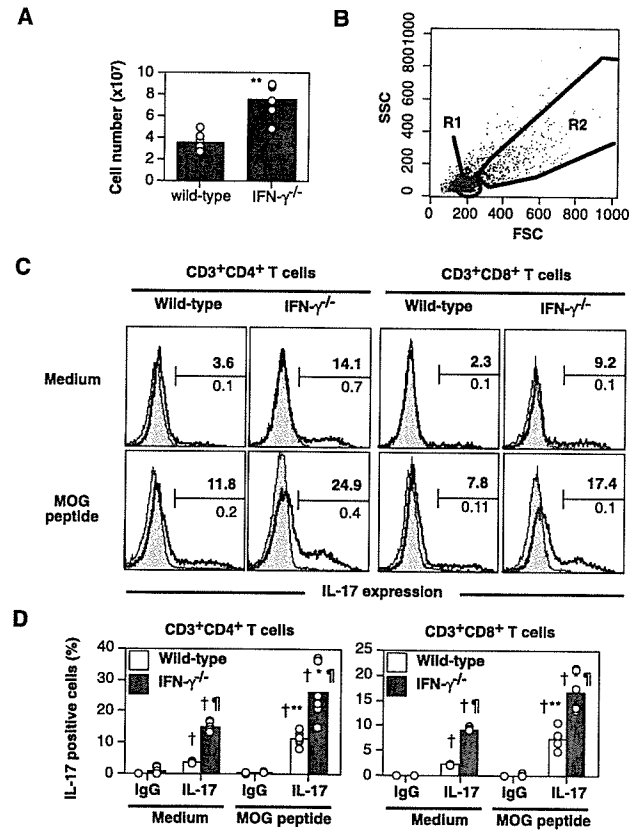

FIGURE 7. The proportion of IL-17-producing $CD4^+$ and $CD8^+$ T cells was increased in IFN-$\gamma^{-/-}$ mice after MOG immunization. LN cells from mice immunized with MOG/CFA were cultured for 72 h in the presence or absence of 50 μg/ml MOG peptide. IL-17-producing cells were then analyzed by FACS, and the percentage of IL-$17^+CD3^+CD4^+$ T cells is shown. *A*, Total LN cell number from inguinal and axillary LNs from wild-type ($n = 6$) and IFN-$\gamma^{-/-}$ ($n = 6$) mice. **, $p < 0.01$ vs wild-type mice. *B*, Gating in FACS analysis, R2 rather than R1 contained MOG-specific proliferating cells using CFSE labeling. *C*, Staining of intracellular IL-17 in $CD3^+CD4^+$ or $CD3^+CD8^+$ T cells stimulated with or without MOG peptides. Shaded areas, staining with isotype-matched control Ab; bold lines, anti-mouse IL-17 staining. The percentage of IL-17-positive cells (upper bold figures) and percentage of cells which were stained with an isotype-matched control IgG (lower figures) are shown. *D*, Each circle represents a value from an individual mouse, and the column represents the average for each group in *C*. □, Wild-type mice ($n = 6$). ■, IFN-$\gamma^{-/-}$ mice ($n = 6$). IgG, isotype-matched control IgG staining. IL-17, anti-mouse IL-17 staining. †, $p < 0.05$ vs the corresponding values for control IgG staining. *, $p < 0.05$ and **, $p < 0.01$ vs the corresponding values for the cultures in the absence of MOG peptide (medium alone). ¶, $p < 0.05$ vs the corresponding values of wild-type mice. All *p* values were determined by the Student's *t* test.

of IL-$17^{-/-}$ mice was significantly increased compared with that in wild-type mice after MOG stimulation (Fig. 8). Similar results were also obtained in $CD8^+$ T cells (Fig. 8). Thus, these data suggest that IL-17 production is regulated by IFN-γ while IFN-γ is regulated by IL-17.

Then, we examined whether IL-17 and IFN-γ can directly regulate IFN-γ and IL-17 production, respectively. When purified splenic $CD4^+$ T cells were stimulated with plate-coated anti-CD3 mAb in the presence of various concentration of IL-12, IFN-γ production was enhanced in a dose-dependent manner (Fig. 9*A*). However, IL-17 did not influence IFN-γ production by $CD4^+$ T cells in the absence or presence of IL-12 (Fig. 9, *B* and *C*). IL-23 could promote IL-17 production dose dependently (Fig. 9*D*), while IFN-γ did not show any effects on IL-17 production irrespective of the presence of IL-23 (Fig. 9, *E* and *F*). These observations indicate that IFN-γ or IL-17 cannot directly modulate IL-17 or IFN-γ production.

Increased MOG-specific Ab production in IL-$17^{-/-}$ mice during EAE

To elucidate the role of IL-17 in MOG-specific Ab production, we measured the level of anti-MOG-specific serum Abs in wild-type and IL-$17^{-/-}$ mice during EAE. Before immunization with MOG peptides, the level of MOG-specific IgG was very low in both wild-type and IL-$17^{-/-}$ mice (Fig. 10*A*). On day 20 after MOG/CFA immunization with PTx injection as shown in Fig. 1, the level of MOG-specific IgG in IL-$17^{-/-}$ mice was slightly higher than that in wild-type mice (Fig. 10*A*). In chronic inflammatory phases during EAE induced by MOG/CFA with PTx, the levels of MOG-specific IgG and IgG1 in IL-$17^{-/-}$ mice were profoundly increased compared with these in wild-type mice, although these IL-$17^{-/-}$ mice did not show any sign of EAE (Fig. 10). Similarly, the levels of MOG-specific IgG2a and IgG2b were also slightly, but not significantly, increased in IL-$17^{-/-}$ mice, while those of MOG-specific IgG3 and IgM were not different between wild-type and IL-$17^{-/-}$ mice (Fig. 10*B*). These results indicated that IL-17 has an influence upon MOG-specific Ab production by B cells. However, our findings suggest that no correlation exists between the susceptibility and severity of EAE and the levels of anti-MOG Abs in IL-$17^{-/-}$ mice.

Discussion

In this study, we have demonstrated using IL-$17^{-/-}$ mice that IL-17 plays an important role in the development of EAE induced by MOG/CFA. We found that, upon immunization with MOG/CFA, T cell sensitization was defective in IL-$17^{-/-}$ mice, and $CD4^+$ T cells from IL-$17^{-/-}$ mice did not induce EAE efficiently compared with wild-type T cells. These observations suggest that IL-17 plays an important role in the activation of encephalitogenic T cells during the sensitization phase of EAE. In contrast, it was recently reported that IL-17-producing $CD4^+$ T cells enhance the

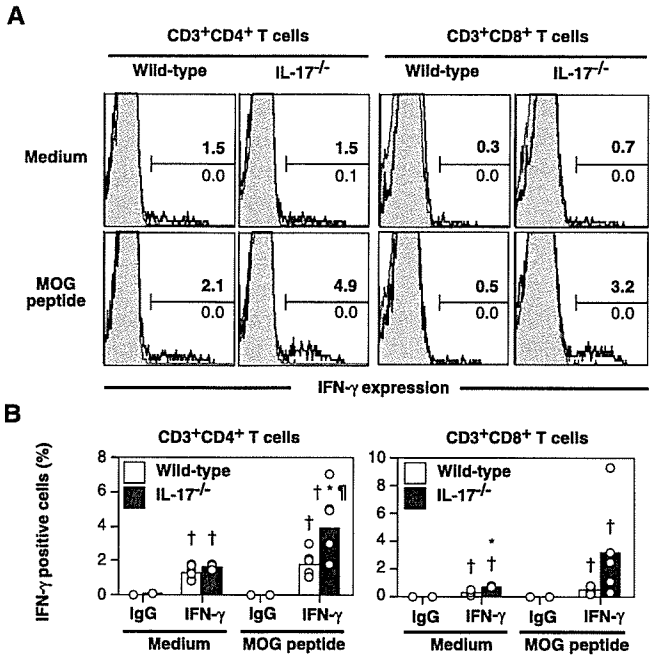

FIGURE 8. The proportion of IFN-γ-producing $CD4^+$ and $CD8^+$ T cells was increased in IL-$17^{-/-}$ mice after MOG immunization. LN cells from mice immunized with MOG/CFA were cultured for 72 h in the presence or absence of 50 μg/ml MOG peptide. IFN-γ-producing cells were then analyzed by FACS, and the percentage of IFN-$\gamma^+CD3^+CD4^+$ or $CD3^+CD8^+$ T cells is shown. *A*, Staining of intracellular IFN-γ in $CD3^+CD4^+$ or $CD3^+CD8^+$ T cells stimulated with or without MOG peptides. Shaded areas, staining with isotype-matched control Ab; bold lines, anti-mouse IFN-γ staining. The percentage of IFN-γ-positive cells (upper bold figures) and percentage of cells which were stained with an isotype-matched control IgG (lower figures) are shown. *B*, Each circle represents a value from an individual mouse, and the column represents the average for each group in *A*. □, Wild-type mice ($n = 6$). ■, IL-$17^{-/-}$ mice ($n = 6$). IgG, isotype-matched control IgG staining. IFN-γ, anti-mouse IFN-γ staining. †, $p < 0.05$ vs the corresponding values for control IgG staining. *, $p < 0.05$ vs the corresponding values for the cultures in the absence of MOG peptide (medium alone). ¶, $p < 0.05$ vs the corresponding values of wild-type mice. All p values were determined by the Student t test.

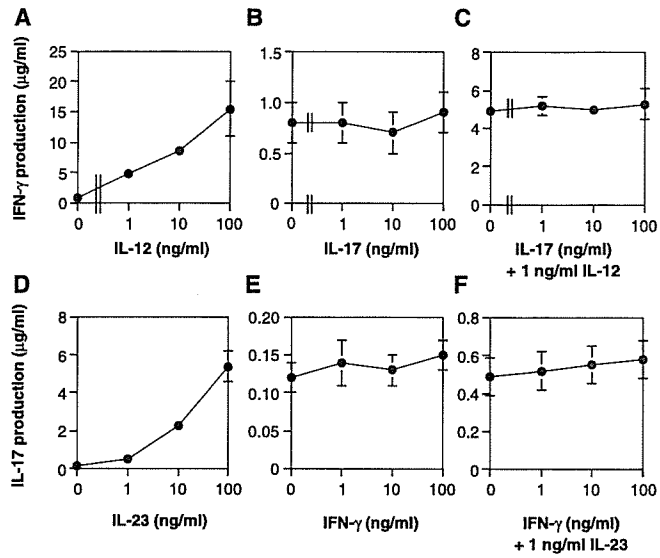

FIGURE 9. Exogenous IFN-γ and IL-17 did not directly affect IL-17 and IFN-γ production by $CD4^+$ T cells. $CD4^+$ T cells from spleen of wild-type mice were stimulated with plate-coated anti-CD3 mAb in the presence or absence of rmIL-17 or rmIFN-γ with or without rmIL-12 or rmIL-23 for 48 h. Then, IFN-γ or IL-17 levels in culture supernatants were determined by ELISA. IFN-γ levels in culture supernatants from $CD4^+$ T cells: stimulated with anti-CD3 mAb plus the indicated amount of rmIL-12 (*A*), rmIL-17 (*B*), and 1 ng/ml rmIL-12 + indicated amount of rmIL-17 (*C*). IL-17 levels in culture supernatants from $CD4^+$ T cells: stimulated with anti-CD3 mAb plus rmIL-23 (*D*), rmIFN-γ (*E*), or 1 ng/ml rmIL-23 + indicated amount of rmIFN-γ (*F*). Data showed the average ± SD from three mice, and a representative result from two independent experiments.

disease severity of EAE and that treatment with anti-IL-17 neutralizing Abs during the elicitation phase suppressed disease development (26). These observations strongly suggest that IL-17 is involved in the pathogenesis of EAE during both the sensitization and elicitation phases.

As Th1 cells, which are the major producers of IFN-γ, infiltrate the inflamed lesions of EAE or collagen-induced arthritis (CIA) (27, 28), it was suspected that IFN-γ may have a pathological role in the development of these autoimmune diseases. However, administration of neutralizing Abs for IFN-γ leads to exacerbation of these diseases (29). The development of CIA is enhanced in IFN-$\gamma^{-/-}$ mice and that of EAE is also exacerbated in both IFN-$\gamma^{-/-}$ and IFN-$\gamma R^{-/-}$ mice compared with wild-type mice (22–25). Thus, IFN-γ may have a protective role in these diseases, rather than a pathogenic role. Consistent with this notion, the development of EAE is also exacerbated in mice deficient for IL-12 p35, a subunit of IL-12 that is required for the differentiation of IFN-γ-producing Th1 cells (30, 31). In a similar manner, the severity of EAE was exaggerated in mice deficient in IL-12Rβ2. Interestingly, we found that the IL-17-producing T cell population was increased in IFN-$\gamma^{-/-}$ mice in comparison to that seen in wild-type mice upon immunized with MOG/CFA (Fig. 7). Similar observations were also currently reported by other groups (32, 33). IL-17 production was also augmented in the splenocytes of IL-12Rβ$2^{-/-}$ mice (20). These observations suggest that IFN-γ plays a beneficial role during the development of EAE by regulating IL-17 production. However, we demonstrated that IFN-γ did not directly influence IL-17 production by $CD4^+$ T cells (Fig. 9, *E* and *F*), suggesting that the suppressive effect of IFN-γ on IL-17 production may be due to the suppression of the development of IL-17-producing cells. In this context, it was recently reported that IL-17-producing cells are induced by IL-23, while IL-12/IFN-γ suppresses the production of IL-17 (34).

We also found that IFN-γ-producing $CD4^+$ and $CD8^+$ T cells were markedly increased in IL-$17^{-/-}$ mice stimulated with MOG peptides, although IL-17 did not show any direct effect on IFN-γ production by $CD4^+$ T cells (Fig. 9, *B* and *C*) (Fig. 8). These observations suggest that IL-17 negatively regulates the development of IFN-γ-producing Th1 cells. Thus, IL-17 and IFN-γ may mutually regulate the development of these cytokine producer cells during immune responses.

We demonstrated that $CD4^+$ T cells are the predominant producers of IL-17 in LN cells after immunization with MOG/CFA. It has been reported that, in Lyme arthritis, IL-17 is primarily produced by a specific subpopulation of $CD4^+$ T cells that are neither Th1 nor Th2 and that produce TNF-α and/or GM-CSF simultaneously. As IL-17 is produced by multiple cell types, including $CD8^+$ T cells, γδ T cells, neutrophils, and eosinophils under different conditions (13–18, 35), the production of IL-17 is not limited to a specific T cell population. Instead, the producer cells in a particular disease appear to be defined by a specific cell population. The mechanism by which these IL-17 producer cells are controlled in different diseases, however, remains to be elucidated.

In MS patients, elevation of anti-MOG Ab levels is detectable in cerebrospinal fluid (36, 37). In association with the elevation of

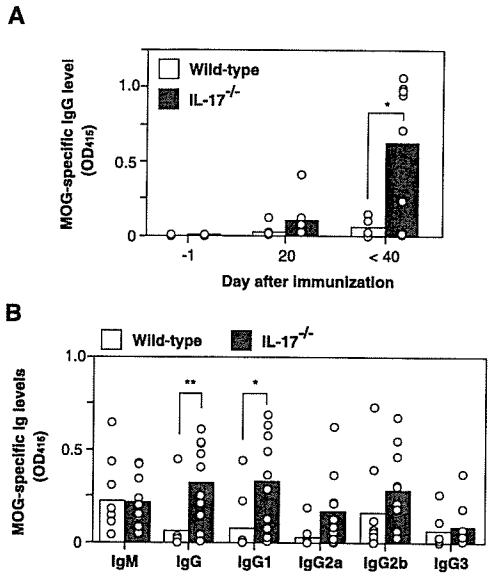

FIGURE 10. Enhanced MOG-specific Ig production in IL-17$^{-/-}$ mice during EAE. MOG-specific Ig levels in sera from wild-type and IL-17$^{-/-}$ mice that developed EAE were determined by ELISA. *A*, As performed in Fig. 1*A*, sera were collected from mice before (−1 day) and after MOG immunization (20 and <40 days). Then, MOG-specific IgG levels in sera were measured. *B*, On day 42 after MOG immunization, MOG-specific IgM, IgG, IgG1, IgG2a, IgG2b, and IgG3 levels in sera were determined. Each circle represents the value from an individual mouse, and a column shows the average of each group. □, Wild-type mice (n = 7). ■, IL-17$^{-/-}$ mice (n = 10). *, $p < 0.05$ and **, $p < 0.01$ for the comparisons shown in brackets by Student's t test.

anti-MOG Abs following immunization with MOG peptides (38), severe demyelination occurred in the Lewis rat, suggesting that the generation of myelin-specific Abs may be involved in the development of EAE. However, we observed that anti-MOG Ab levels were increased in IL-17$^{-/-}$ mice in comparison with the levels seen in wild-type mice after immunization with MOG, while the development of EAE was markedly suppressed in IL-17$^{-/-}$ mice (Fig. 10). Thus, in IL-17$^{-/-}$ mice, there is no apparent correlation between the severity of EAE and the elevation of anti-MOG Abs in IL-17$^{-/-}$ mice, suggesting that anti-MOG Abs are not directly involved in the development of this disease. In fact, the serum MOG-specific Ab levels in mice that developed EAE after the transfer of MOG-specific CD4$^+$ T cells were below the limits of detection (data not shown). In support of this notion, B cell-deficient mice develop EAE normally (39–41). It was reported, however, that Abs are involved in the remyelination of the lesions in the CNS during disease resolution (42). We did not expect that Ab levels specific for MOG would be enhanced in IL-17$^{-/-}$ mice, because Ab production was suppressed in IL-17$^{-/-}$ mice during CIA and contact, delayed-type, and airway hypersensitivity (9–11). We do not currently understand the reasoning for this. The molecular nature of the Ags involved in the autoimmune disorders, however, appears to affect the sensitivity of the disease to IL-17. Additional experiments will be necessary to elucidate the mechanism.

We previously reported that IL-17 is not essential for the induction of graft-vs-host reaction (GVHR) (9), in which CD8$^+$ T cell-derived FasL and perforin play important roles (43, 44). Likewise, IL-17-deficiency did not affect the incidence of hyperglycemia in NOD mice (T. Matsuki, S. Nakae, and Y. Iwakura, unpublished observations), although IL-17 mRNA expression is increased in NOD mice upon development of insulin-dependent diabetes mellitus (IDDM) (45). In this case, CD8$^+$ cells, rather than CD4$^+$ cells, are also suggested to be involved in the apoptosis of β cells in the pancreatic Langerhans islands (46, 47). In both cases, IFN-γ is involved in the pathogenesis of the diseases (48, 49) (50). Thus, these observations indicate that these two types of inflammatory responses are clearly different; EAE and CIA are IL-17 dependent, and IL-17-producing cells play a major role, while IDDM and GVHR are IFN-γ dependent, and CD8$^+$ cytotoxic T cells and/or CD4$^+$ Th1 cells play important roles.

Taken together, our data demonstrate that IL-17 and IFN-γ, produced by a distinct population of T cells, have different roles in the development of EAE, CIA, GVHR, and hyperglycemia. These results suggest that these cytokines may also be involved in the development of MS, RA, GVHD, and IDDM in humans. Elucidation of the roles of pathogenic cytokines and the mechanisms of cytokine dependency may provide potential targets for novel therapeutics to treat these diseases.

Acknowledgments

We thank Dr. S. J. Galli (Stanford University School of Medicine, Stanford, CA) for his generous support for this study. We also thank Tomoko Hata and Hayato Kotaki for their excellent animal care.

Disclosures

The authors have no financial conflict of interest.

References

1. Moseley, T. A., D. R. Haudenschild, L. Rose, and A. H. Reddi. 2003. Interleukin-17 family and IL-17 receptors. *Cytokine Growth Factor Rev.* 14: 155–174.
2. Chabaud, M., J. M. Durand, N. Buchs, F. Fossiez, G. Page, L. Frappart, and P. Miossec. 1999. Human interleukin-17: A T cell-derived proinflammatory cytokine produced by the rheumatoid synovium. *Arthritis Rheum.* 42: 963–970.
3. Wong, C. K., C. Y. Ho, E. K. Li, and C. W. Lam. 2000. Elevation of proinflammatory cytokine (IL-18, IL-17, IL-12) and Th2 cytokine (IL-4) concentrations in patients with systemic lupus erythematosus. *Lupus* 9: 589–593.
4. Hamzaoui, K., A. Hamzaoui, F. Guemira, M. Bessioud, M. Hamza, and K. Ayed. 2002. Cytokine profile in Behcet's disease patients: relationship with disease activity. *Scand. J. Rheumatol.* 31: 205–210.
5. Antonysamy, M. A., W. C. Fanslow, F. Fu, W. Li, S. Qian, A. B. Troutt, and A. W. Thomson. 1999. Evidence for a role of IL-17 in organ allograft rejection: IL-17 promotes the functional differentiation of dendritic cell progenitors. *J. Immunol.* 162: 577–584.
6. Matsumoto, K., and K. Kanmatsuse. 2002. Increased urinary excretion of interleukin-17 in nephrotic patients. *Nephron* 91: 243–249.
7. Wong, C. K., C. Y. Ho, F. W. Ko, C. H. Chan, A. S. Ho, D. S. Hui, and C. W. Lam. 2001. Proinflammatory cytokines (IL-17, IL-6, IL-18 and IL-12) and Th cytokines (IFN-γ, IL-4, IL-10 and IL-13) in patients with allergic asthma. *Clin. Exp. Immunol.* 125: 177–183.
8. Lock, C., G. Hermans, R. Pedotti, A. Brendolan, E. Schadt, H. Garren, A. Langer-Gould, S. Strober, B. Cannella, J. Allard, et al. 2002. Gene-microarray analysis of multiple sclerosis lesions yields new targets validated in autoimmune encephalomyelitis. *Nat. Med.* 8: 500–508.
9. Nakae, S., Y. Komiyama, A. Nambu, K. Sudo, M. Iwase, I. Homma, K. Sekikawa, M. Asano, and Y. Iwakura. 2002. Antigen-specific T cell sensitization is impaired in IL-17-deficient mice, causing suppression of allergic cellular and humoral responses. *Immunity* 17: 375–387.
10. Nakae, S., A. Nambu, K. Sudo, and Y. Iwakura. 2003. Suppression of immune induction of collagen-induced arthritis in IL-17-deficient mice. *J. Immunol.* 171: 6173–6177.
11. Nakae, S., S. Saijo, R. Horai, K. Sudo, S. Mori, and Y. Iwakura. 2003. IL-17 production from activated T cells is required for the spontaneous development of destructive arthritis in mice deficient in IL-1 receptor antagonist. *Proc. Natl. Acad. Sci. USA* 100: 5986–5990.
12. Ye, P., F. H. Rodriguez, S. Kanaly, K. L. Stocking, J. Schurr, P. Schwarzenberger, P. Oliver, W. Huang, P. Zhang, J. Zhang, et al. 2001. Requirement of interleukin 17 receptor signaling for lung CXC chemokine and granulocyte colony-stimulating factor expression, neutrophil recruitment, and host defense. *J. Exp. Med.* 194: 519–527.
13. Aarvak, T., M. Chabaud, P. Miossec, and J. B. Natvig. 1999. IL-17 is produced by some proinflammatory Th1/Th0 cells but not by Th2 cells. *J. Immunol.* 162: 1246–1251.
14. Albanesi, C., C. Scarponi, A. Cavani, M. Federici, F. Nasorri, and G. Girolomoni. 2000. Interleukin-17 is produced by both Th1 and Th2 lymphocytes, and modulates interferon-γ- and interleukin-4-induced activation of human keratinocytes. *J. Invest. Dermatol.* 115: 81–87.
15. Infante-Duarte, C., H. F. Horton, M. C. Byrne, and T. Kamradt. 2000. Microbial lipopeptides induce the production of IL-17 in Th cells. *J. Immunol.* 165: 6107–6115.

16. Molet, S., Q. Hamid, F. Davoine, E. Nutku, R. Taha, N. Page, R. Olivenstein, J. Elias, and J. Chakir. 2001. IL-17 is increased in asthmatic airways and induces human bronchial fibroblasts to produce cytokines. *J. Allergy Clin. Immunol.* 108: 430–438.
17. Ferretti, S., O. Bonneau, G. R. Dubois, C. E. Jones, and A. Trifilieff. 2003. IL-17, produced by lymphocytes and neutrophils, is necessary for lipopolysaccharide-induced airway neutrophilia: IL-15 as a possible trigger. *J. Immunol.* 170: 2106–2112.
18. Happel, K. I., M. Zheng, E. Young, L. J. Quinton, E. Lockhart, A. J. Ramsay, J. E. Shellito, J. R. Schurr, G. J. Bagby, S. Nelson, and J. K. Kolls. 2003. Roles of Toll-like receptor 4 and IL-23 in IL-17 expression in response to *Klebsiella pneumoniae* infection. *J. Immunol.* 170: 4432–4436.
19. Matusevicius, D., P. Kivisakk, B. He, N. Kostulas, V. Ozenci, S. Fredrikson, and H. Link. 1999. Interleukin-17 mRNA expression in blood and CSF mononuclear cells is augmented in multiple sclerosis. *Mult. Scler.* 5: 101–104.
20. Zhang, G. X., B. Gran, S. Yu, J. Li, I. Siglienti, X. Chen, M. Kamoun, and A. Rostami. 2003. Induction of experimental autoimmune encephalomyelitis in IL-12 receptor-β2-deficient mice: IL-12 responsiveness is not required in the pathogenesis of inflammatory demyelination in the central nervous system. *J. Immunol.* 170: 2153–2160.
21. Kassiotis, G., K. Kranidioti, and G. Kollias. 2001. Defective CD4T cell priming and resistance to experimental autoimmune encephalomyelitis in TNF-deficient mice due to innate immune hypo-responsiveness. *J. Neuroimmunol.* 119: 239–247.
22. Ferber, I. A., S. Brocke, C. Taylor-Edwards, W. Ridgway, C. Dinisco, L. Steinman, D. Dalton, and C. G. Fathman. 1996. Mice with a disrupted IFN-γ gene are susceptible to the induction of experimental autoimmune encephalomyelitis (EAE). *J. Immunol.* 156: 5–7.
23. Willenborg, D. O., S. Fordham, C. C. Bernard, W. B. Cowden, and I. A. Ramshaw. 1996. IFN-γ plays a critical down-regulatory role in the induction and effector phase of myelin oligodendrocyte glycoprotein-induced autoimmune encephalomyelitis. *J. Immunol.* 157: 3223–3227.
24. Chu, C. Q., S. Wittmer, and D. K. Dalton. 2000. Failure to suppress the expansion of the activated CD4 T cell population in interferon γ-deficient mice leads to exacerbation of experimental autoimmune encephalomyelitis. *J. Exp. Med.* 192: 123–128.
25. Krakowski, M., and T. Owens. 1996. Interferon-γ confers resistance to experimental allergic encephalomyelitis. *Eur. J. Immunol.* 26: 1641–1646.
26. Langrish, C. L., Y. Chen, W. M. Blumenschein, J. Mattson, B. Basham, J. D. Sedgwick, T. McClanahan, R. A. Kastelein, and D. J. Cua. 2005. IL-23 drives a pathogenic T cell population that induces autoimmune inflammation. *J. Exp. Med.* 201: 233–240.
27. Traugott, U., and P. Lebon. 1988. Demonstration of α, β, and γ interferon in active chronic multiple sclerosis lesions. *Ann. NY Acad. Sci.* 540: 309–311.
28. Hammarberg, H., O. Lidman, C. Lundberg, S. Y. Eltayeb, A. W. Gielen, S. Muhallab, A. Svenningsson, H. Linda, P. H. van Der Meide, S. Cullheim, et al. 2000. Neuroprotection by encephalomyelitis: rescue of mechanically injured neurons and neurotrophin production by CNS-infiltrating T and natural killer cells. *J. Neurosci.* 20: 5283–5291.
29. Begolka, W. S., and S. D. Miller. 1998. Cytokines as intrinsic and exogenous regulators of pathogenesis in experimental autoimmune encephalomyelitis. *Res. Immunol.* 149: 771–781; discussion 843; 774: 855–760.
30. Becher, B., B. G. Durell, and R. J. Noelle. 2002. Experimental autoimmune encephalitis and inflammation in the absence of interleukin-12. *J. Clin. Invest.* 110: 493–497.
31. Gran, B., G. X. Zhang, S. Yu, J. Li, X. H. Chen, E. S. Ventura, M. Kamoun, and A. Rostami. 2002. IL-12p35-deficient mice are susceptible to experimental autoimmune encephalomyelitis: evidence for redundancy in the IL-12 system in the induction of central nervous system autoimmune demyelination. *J. Immunol.* 169: 7104–7110.
32. Park, H., Z. Li, X. O. Yang, S. H. Chang, R. Nurieva, Y. H. Wang, Y. Wang, L. Hood, Z. Zhu, Q. Tian, and C. Dong. 2005. A distinct lineage of CD4 T cells regulates tissue inflammation by producing interleukin 17. *Nat. Immunol.* 6: 1133–1141.
33. Harrington, L. E., R. D. Hatton, P. R. Mangan, H. Turner, T. L. Murphy, K. M. Murphy, and C. T. Weaver. 2005. Interleukin 17-producing $CD4^+$ effector T cells develop via a lineage distinct from the T helper type 1 and 2 lineages. *Nat. Immunol.* 6: 1123–1132.
34. Aggarwal, S., N. Ghilardi, M. H. Xie, F. J. de Sauvage, and A. L. Gurney. 2003. Interleukin-23 promotes a distinct CD4 T cell activation state characterized by the production of interleukin-17. *J. Biol. Chem.* 278: 1910–1914.
35. Umemura, M., T. Kawabe, K. Shudo, H. Kidoya, M. Fukui, M. Asano, Y. Iwakura, G. Matsuzaki, R. Imamura, and T. Suda. 2004. Involvement of IL-17 in Fas ligand-induced inflammation. *Int. Immunol.* 16: 1099–1108.
36. Xiao, B. G., C. Linington, and H. Link. 1991. Antibodies to myelin-oligodendrocyte glycoprotein in cerebrospinal fluid from patients with multiple sclerosis and controls. *J. Neuroimmunol.* 31: 91–96.
37. Sun, J., H. Link, T. Olsson, B. G. Xiao, G. Andersson, H. P. Ekre, C. Linington, and P. Diener. 1991. T and B cell responses to myelin-oligodendrocyte glycoprotein in multiple sclerosis. *J. Immunol.* 146: 1490–1495.
38. Ichikawa, M., T. G. Johns, J. Liu, and C. C. Bernard. 1996. Analysis of the fine B cell specificity during the chronic/relapsing course of a multiple sclerosis-like disease in Lewis rats injected with the encephalitogenic myelin oligodendrocyte glycoprotein peptide 35–55. *J. Immunol.* 157: 919–926.
39. Wolf, S. D., B. N. Dittel, F. Hardardottir, and C. A. Janeway, Jr. 1996. Experimental autoimmune encephalomyelitis induction in genetically B cell-deficient mice. *J. Exp. Med.* 184: 2271–2278.
40. Hjelmstrom, P., A. E. Juedes, J. Fjell, and N. H. Ruddle. 1998. B-cell-deficient mice develop experimental allergic encephalomyelitis with demyelination after myelin oligodendrocyte glycoprotein sensitization. *J. Immunol.* 161: 4480–4483.
41. Dittel, B. N., T. H. Urbania, and C. A. Janeway, Jr. 2000. Relapsing and remitting experimental autoimmune encephalomyelitis in B cell deficient mice. *J. Autoimmun.* 14: 311–318.
42. Hunter, S. F., D. J. Miller, and M. Rodriguez. 1997. Monoclonal remyelination-promoting natural autoantibody SCH 94.03: pharmacokinetics and in vivo targets within demyelinated spinal cord in a mouse model of multiple sclerosis. *J. Neurol. Sci.* 150: 103–113.
43. Baker, M. B., N. H. Altman, E. R. Podack, and R. B. Levy. 1996. The role of cell-mediated cytotoxicity in acute GVHD after MHC-matched allogeneic bone marrow transplantation in mice. *J. Exp. Med.* 183: 2645–2656.
44. Brochu, S., B. Rioux-Masse, J. Roy, D. C. Roy, and C. Perreault. 1999. Massive activation-induced cell death of alloreactive T cells with apoptosis of bystander postthymic T cells prevents immune reconstitution in mice with graft-versus-host disease. *Blood* 94: 390–400.
45. Vukkadapu, S. S., J. M. Belli, K. Ishii, A. G. Jegga, J. J. Hutton, B. J. Aronow, and J. D. Katz. 2005. Dynamic interaction between T cell-mediated β cell damage and β cell repair in the run-up to autoimmune diabetes of the NOD mouse. *Physiol. Genomics* 21: 201–211.
46. Kagi, D., B. Odermatt, P. Seiler, R. M. Zinkernagel, T. W. Mak, and H. Hengartner. 1997. Reduced incidence and delayed onset of diabetes in perforin-deficient nonobese diabetic mice. *J. Exp. Med.* 186: 989–997.
47. Itoh, N., A. Imagawa, T. Hanafusa, M. Waguri, K. Yamamoto, H. Iwahashi, M. Moriwaki, H. Nakajima, J. Miyagawa, M. Namba, et al. 1997. Requirement of Fas for the development of autoimmune diabetes in nonobese diabetic mice. *J. Exp. Med.* 186: 613–618.
48. Hultgren, B., X. Huang, N. Dybdal, and T. A. Stewart. 1996. Genetic absence of γ-interferon delays but does not prevent diabetes in NOD mice. *Diabetes* 45: 812–817.
49. Wang, B., I. Andre, A. Gonzalez, J. D. Katz, M. Aguet, C. Benoist, and D. Mathis. 1997. Interferon-γ impacts at multiple points during the progression of autoimmune diabetes. *Proc. Natl. Acad. Sci. USA* 94: 13844–13849.
50. Ellison, C. A., J. M. Fischer, K. T. HayGlass, and J. G. Gartner. 1998. Murine graft-versus-host disease in an F_1-hybrid model using IFN-γ gene knockout donors. *J. Immunol.* 161: 631–640.

Signaling of vascular endothelial growth factor receptor-1 tyrosine kinase promotes rheumatoid arthritis through activation of monocytes/macrophages

Masato Murakami, Shinobu Iwai, Sachie Hiratsuka, Mai Yamauchi, Kazuhide Nakamura, Yoichiro Iwakura, and Masabumi Shibuya

Vascular endothelial growth factor (VEGF) and VEGF receptor-1 (VEGFR-1/Flt-1) were shown to be involved in pathological angiogenesis, particularly rheumatoid arthritis (RA). However, the molecular basis of their actions is not fully understood. Here we report that in a murine model of RA, deletion of the tyrosine kinase (TK) domain of VEGFR-1 decreased the incidence and clinical symptoms of RA. Pathological symptoms, such as synovial hyperplasia, inflammatory infiltrates, pannus formation, and cartilage/bone destruction, became milder in *Vegfr-1 tk*$^{-/-}$ mice compared with wild-type (Wt) mice in the human T-cell leukemia virus-1 *(HTLV-1) pX*–induced chronic models. VEGFR-1 TK-deficient bone marrow cells showed a suppression of multilineage colony formation. Furthermore, macrophages induced to differentiate in vitro showed a decrease in immunologic reactions such as phagocytosis and the secretion of interleukin-6 (IL-6) and VEGF-A. Treatment of this RA model with a small molecule inhibitor for VEGFR TK, KRN951, also attenuated the arthritis. These results indicate that the VEGFR-1 TK signaling modulates the proliferation of bone marrow hematopoietic cells and immunity of monocytes/macrophages and promotes chronic inflammation, which may be a new target in the treatment of RA. (Blood. 2006;108:1849-1856)

Introduction

Vascular endothelial growth factors (VEGFs) and their receptors (VEGFRs), including VEGFR-1 (Flt-1), VEGFR-2 (KDR/Flk-1), and VEGFR-3 (Flt-4), form a regulatory system crucial for normal development and pathological angiogenesis.[1-4] VEGFRs are structurally related to the Fms/Kit/PDGFR family and contain an extracellular domain carrying 7 immunoglobulin (Ig)–like repeats and a cytoplasmic tyrosine kinase (TK) domain.[5,6] VEGFR-1 and VEGFR-2 are highly expressed on vascular endothelial cells.[7-10] We and others have recently shown that VEGFR-1 is expressed not only in vascular endothelial cells but also in monocytes/macrophages,[11,12] and its signaling is involved in the migration of macrophages toward VEGF-A.[13] In addition to VEGF-A, VEGF-B and PlGF are also ligands for VEGFR-1; thus, they could play a role in this signaling under both physiological and pathological conditions. Other nonendothelial cells, including smooth muscle cells, trophoblasts, and osteoblasts, were reported to express VEGFR-1.[14]

Mice lacking *Vegfr-2* die in the embryonic stage due to a severe deficiency of vascular development.[15] In contrast, mice lacking *Vegfr-1* die due to overgrowth and disorganization of the vascular system.[16] Interestingly, however, mouse embryos lacking the TK domain of *Vegfr-1* survive without significant defects,[17] suggesting that VEGFR-1 functions as a negative regulator of vascular development by trapping VEGF-A via its ligand-binding domain.[14] Recently, various studies including ours indicated that the expression of VEGFs and VEGFRs is up-regulated in various diseases.[2,4,18-20] VEGFR-1–mediated signaling was shown to play a significant role in a variety of pathological conditions such as carcinogenesis and inflammatory diseases.[19,21,22] VEGFR-1 signaling facilitates tumor angiogenesis and spontaneous lung metastases by inducing the expression of matrix metalloproteinase 9 (MMP-9).[22-24] A recent study also showed that VEGFR-1 is important for the reconstitution of hematopoiesis in bone marrow (BM) after irradiation.[25]

Rheumatoid arthritis (RA)[26] is a chronic systemic disease characterized by an inflammatory erosive synovitis, which shows marked neovascularization, inflammatory cell infiltration, and synovial hyperplasia. These pathological reactions gradually induce a pannus, with inflammatory vascular tissue leading to an irreversible loss of cartilage and bone.[27,28] VEGF-A is highly expressed in synovial fluid in RA.[29] Immunohistochemical and in situ hybridization studies on the synovial tissues have shown that VEGF-A is strongly expressed in synovial macrophages, fibroblasts surrounding microvessels, and vascular smooth muscle cells.[29,30] In inflamed joints, many cytokines, including VEGF and the proinflammatory interleukin-1 (IL-1), IL-6, and tumor

From the Division of Genetics and Division of Cell Biology, Center for Experimental Medicine, Institute of Medical Science, University of Tokyo, Japan; Department of Pharmacology, Tokyo Women's Medical University, Japan; and Pharmaceutical Developmental Laboratories, Kirin Brewery, Gunma, Japan.

Submitted December 21, 2005; accepted May 1, 2006. Prepublished online as *Blood* First Edition Paper, May 18, 2006; DOI 10.1182/blood-2006-04-016030.

Supported by Grant-in-Aid Special Project Research on Cancer-Bioscience 12215024 from the Ministry of Education, Culture, Sports, Science and Technology in Japan; a grant for the program "Research for the Future" from the Japan Society for Promotion of Science; and the program "Promotion of Fundamental Research in Health Science" from the Organization for Pharmaceutical Safety and Research (OPSR).

M.M., Y.I., and M.S. participated in designing the research; M.M., S.I., and M.Y. performed the research; M.M. centralized the pathological review and analyzed data; S.H. and Y.I provided gene-targeting mice; K.N. provided new reagents; M.M. and M.S. wrote the manuscript; and all authors checked the final version of the manuscript.

The online version of the article contains a data supplement.

Reprints: Masabumi Shibuya, Division of Genetics, Institute of Medical Science, University of Tokyo, 4-6-1, Shirokane-dai, Minato-ku, Tokyo, 108-8639, Japan; e-mail: shibuya@ims.u-tokyo.ac.jp.

The publication costs of this article were defrayed in part by page charge payment. Therefore, and solely to indicate this fact, this article is hereby marked "advertisement" in accordance with 18 U.S.C. section 1734.

necrosis factor-α (TNF-α), play important roles in the pathogenesis of RA.[31]

Iwakura et al have recently reported that the human T-cell leukemia virus-1 *(HTLV-1) pX* transgenic mouse is a useful model for studying RA[32] in that it is more similar to human RA than other models, such as collagen-antibody–induced arthritis, in terms of chronic progression, the production of rheumatoid factor, and pathological findings.[33] Interesting characteristics of *pX* transgenic mice include a high incidence of arthritis in the BALB/c genetic background[34] and up-regulation of the production of cytokines such as IL-6 and TNF-α.[35] However, it is not clear yet how the signaling of VEGFR-1 is involved in *pX*-induced or anticollagen-antibody–induced RA.

In this study, we examined these points using wild-type and *Vegfr-1 tk*–deficient mice. We have found that in *Vegfr-1 tk*$^{-/-}$ mice, the arthritis was significantly suppressed through a decrease in the inflammatory response of monocytes/macrophages and hematopoietic proliferation.

Materials and methods

Mice and the marker-assisted selection protocol (MASP)

All the experiments using animal models were carried out according to the guidelines set by the Animal Center of The Institute of Medical Science, The University of Tokyo. To obtain *Vegfr-1 tk*$^{-/-}$ mice with the BALB/c background, we backcrossed *Vegfr-1 tk*$^{+/-}$ heterozygous males (original genetic background is 50% 129SV and 50% C57BL/6) with BALB/c females using marker-assisted selection protocol (MASP) (speed congenics). First, a total of 60 polymorphic polymerase chain reaction (PCR)–based microsatellite loci were randomly obtained from Mouse Genome Informatics of The Jackson Laboratory[36] (Table S1, available on the *Blood* website; see the Supplemental Materials link at the top of the online article). Two to 6 markers were set for each chromosome with an average spacing of 20 cM. At every generation, the mouse carrying the fewest C57BL/6 background loci was used for backcrossing. After 4 generations, less than 3% of C57BL/6 background loci were left, and then crosses were made with *pX* transgenic mice to compare the incidence of arthritis in newly prepared congenic mice with that in the control *pX* mice. Finally, *pX Vegfr-1 tk*$^{+/-}$ mice were crossed with *Vegfr-1 tk*$^{+/-}$ mice for the experiments (Figure 1B).

For the *pX*-induced arthritis, animals were observed every month from age 2 to 6 months and then killed for assessment. For the collagen-antibody–induced arthritis, 8-week-old BALB/c female *Vegfr-1 tk*$^{-/-}$ and wild-type mice were used. Acute arthritis was induced by the intraperitoneal injection of 1 mg of an antitype II collagen–monoclonal antibody cocktail (Chondrex, Redmond, WA) on day 0 followed by the intraperitoneal injection of 50 μg lipopolysaccharide (LPS) on day 3. Animals were killed for assessment on day 7.

Arthritis and histologic score

The incidence and severity of arthritis were examined monthly for *pX* mice and daily for mice with collagen-antibody–induced arthritis by qualitative clinical scoring as follows: 0, normal; 1, mild redness and swelling of the ankle or wrist; 2, moderate redness and swelling; 3, severe redness and swelling of the entire paw; 4, maximally inflamed limb within multiple joints. The number of joints observed was 33 to 122 for each genotype and each month. Mice were killed by neck dislocation, and joints were fixed in paraformaldehyde (PFA) and decalcified in EDTA. Then sagittal paw paraffin sections were examined by hematoxylin and eosin (HE) staining and immunohistochemical staining with von Willebrand factor (VWF) antibody (Dakopatts, Glostrup, Denmark). Histologic examination including morphologic analysis was carried out by semiquantitive grade scoring. In brief, for each paw joint, synovial hyperplasia, inflammatory cell infiltration, pannus formation, and bone and cartilage destruction were scored as follows: 0, none; 1, mild; 2, moderate; 3, severe. The sum of the scores for each paw was used as a histologic score index of the 64 paws for *pX* mice and 50 paws for *pX Vegfr-1 tk*$^{-/-}$ mice. The density of VWF-positive vessels in the hyperplasic synovia was determined by measuring the immunoreactive area in 3 chosen paw joints, which had an average grade. Vascular density was analyzed using a Kurabo Angiogenesis Image Analyzer (Kurabo, Osaka, Japan).

Macrophage activities for cytokine secretion and phagocytosis

For the cytokine secretion assay, mouse peritoneal macrophages were collected 3 days after the intraperitoneal injection of 4% thioglycolate. Peritoneal lavage was collected with 0.5% BSA, 2 mM EDTA (pH 7.2), and PBS, washed twice, and purified using anti–mouse CD11b magnetic-activated cell sorting (MACS) (Miltenyi Biotec, Bergisch Gladbach, Germany). The purity of macrophages was more than 90%. About 4×10^5 macrophages in 0.2 mL of 0.1% BSA–RPMI 1640 medium were seeded into a 96-well plate and incubated with recombinant human VEGF-A (hVEGF-A) (100 ng/mL) or control PBS, with or without a VEGFR inhibitor, SU5416[37] or KRN633.[38] After 48 hours of incubation, the supernatants were collected after centrifugation and cytokine concentrations were measured using a mouse IL-6 and VEGF-A enzyme-linked immunosorbent assay (ELISA) kit (R&D Systems, Minneapolis, MN). Total RNA from hVEGF-A–stimulated macrophages after 24 hours of incubation was isolated using an RNeasy Quick spin column (QIAGEN, Hilden, Germany). The total RNA was analyzed using a real-time reverse transcriptase (RT)–PCR according to the manufacturer's instructions (Takara Bio, Shiga, Japan). All the primers used for the amplification are listed in Table S2. For the phagocytosis assay, BM mononuclear cells (BMMNCs) of both *Vegfr-1 tk*$^{-/-}$ and wild-type mice were collected from the femur, and then 3×10^6 cells in 3.0 mL were cultured in 6-well plates with 100 ng/mL M-CSF (R&D Systems) in 10% FCS–RPMI 1640 medium. On days 2 and 5 of culture, nonadherent cells were discarded. On day 7, the confluent monolayers of adherent macrophages were used for the phagocytosis assay. Confluent macrophages were washed twice with cold PBS, resuspended in 1 mL RPMI 1640 medium containing FITC-dextran (Sigma, St Louis, MO) (100 ng/mL) or Alexa LPS (20 ng/mL) (Molecular Probes, Eugene, OR), and incubated for 2 hours at 37°C. After the incubation, plates were immediately transferred onto ice. This was followed by a quick aspiration of the medium and the washing of cells to remove unphagocytosed particles. Adding PFA stopped the phagocytotic reaction. Total fluorescence was measured with a fluorescence-activated cell sorting (FACS) machine Epics-XL (Beckman Coulter, Fullerton CA). The instrument was set to collect 2×10^4 cells, and profiles of phagocytosis were analyzed using FlowJo software (Tree Star, Ashland, OR).

Treatment of arthritis-model mice with a kinase inhibitor

A low-molecular-weight chemical, KRN951, was obtained from the Kirin Brewery (Gunma, Japan). KRN951 is a VEGFR inhibitor suppressing the TK of VEGFR-1, VEGFR-2, and VEGFR-3. Inhibition of the phosphorylation of VEGFR-1 and -2 with KRN951 is shown in Figure S1. KRN951 was dissolved in 0.5% methylcellulose, Metolose SM15 (Shin-Etsu Chemical, Tokyo, Japan). The KRN951 solution was orally administered to mice with *pX*-induced arthritis at 20 mg/kg/d for 5 days a week, with a 2-day rest period, between the age of 8 and 26 weeks. The mice with collagen-antibody–induced arthritis were given the same inhibitor from day 3 to day 7 at 10, 20, and 40 mg/kg/d, respectively. The control solution was 0.5% methylcellulose without the inhibitor.

Colony formation assay

About 1×10^5 BMMNCs per 35-mm plate (triplicate) were cultured in complete methylcellulose containing 50 ng/mL recombinant murine SCF (rmSCF), 10 ng/mL rmIL-3, 10 ng/mL rhIL-6, and 3 U/mL recombinant human erythropoietin (rhEPO) (Stem Cell Technologies, Vancouver, BC, Canada). Colonies were scored and phenotyped on an inverted phase microscope 10 days after seeding.

Flow cytometric analysis of BM cells

Mouse BM cells were isolated by flushing the femur BM tissues with 1% FBS–PBS, and a single-cell suspension was obtained. Remaining red blood cells were removed with lysis buffer (10 mM NH_4Cl). BMMNCs were stained with monoclonal antibodies for Sca-1 (BD Pharmingen, San Diego, CA) and CD34 (BD Pharmingen) and analyzed using a flow cytometer (Epics-XL, Beckman Coulter). The instrument was set to collect 2×10^4 cells, and these cells were analyzed using FlowJo software (Tree Star). All experiments were performed in triplicate.

Statistical analysis

An unpaired Student *t* test was used for all analyses. Differences were considered to be statistically significant for *P* values below .05 and .01.

Results

Speed congenics significantly shorten the period of backcrossing for establishing *Vegfr-1 tk*$^{-/-}$ BALB/c mice

The incidence of arthritis in *pX* transgenic mice is significantly higher in the genetic background of BALB/c than C57BL/6. Because the original genetic background of *Vegfr-1 tk*$^{-/-}$ mice is 50% 129SV and 50% C57BL/6, we prepared BALB/c-background congenic mice carrying the *Vegfr-1 tk*$^{+/-}$ gene. To shorten the crossing time, we used a MASP or speed congenics to establish BALB/c congenic mice (see "Materials and methods"). The mouse showing the least number of C57BL/6-background loci was selected for backcrossing. After 4 generations, less than 3% of the C57BL/6 background was left (Figure 1A). After the speed congenics, *Vegfr-1 tk*$^{+/-}$ BALB/c congenic mice were mated with *pX* BALB/c mice, which generated 4 genotypes (*pX*, *pX Vegfr-1*$^{+/-}$, *Vegfr-1*$^{+/-}$, and wild-type) (Figure 1B).

To confirm that the congenic strain efficiently changed to the BALB/c background, we compared the incidence of arthritis between the original *pX* mice and the newly prepared congenic *pX* mice. The original *pX* mice and the speed congenic BALB/c *pX* mice showed severe arthritis with no difference in the incidence of disease (Figure 1C). After verification, we mated *pX Vegfr-1 tk*$^{+/-}$ and *Vegfr-1 tk*$^{+/-}$ mice to generate the transgenic mice and other mice for the experiments (Figure 1B).

Signals from VEGFR-1 TK contribute to the onset and the progression of arthritis

We measured the incidence and clinical grade of arthritis in the presence or absence of VEGFR-1 TK signals using *pX*, *pX Vegfr-1 tk*$^{+/-}$, and *pX Vegfr-1 tk*$^{-/-}$ mice (Figure 1B). The incidence of arthritis, detected as paw swelling, erythema, and ankylosis, was significantly lower in *pX Vegfr-1 tk*$^{-/-}$ mice than *Vegfr-1* wild-type *pX* transgenic mice at all the stages examined ($P < .072$ at 2 to 6 months) (Figure 2A). In addition, the incidence of arthritis was lower in the heterozygous *Vegfr-1 tk*$^{+/-}$ mice than *pX* transgenic wild-type mice before 4 months of age, although the difference was not statistically significant (Figure 2A). Clinical scores measured based on redness and swelling of the ankle or wrist were also significantly lower in *pX Vegfr-1 tk*$^{-/-}$ mice than *pX* wild-type mice ($P < .058$ at 2 to 6 months). Furthermore, *pX Vegfr-1 tk*$^{+/-}$ mice showed mild clinical scores between those of *pX* mice and *pX Vegfr-1 tk*$^{-/-}$ mice ($P = .025$ to .454 at 2 to 6 months) (Figure 2B).

Next we examined the histologic difference between *pX* mice and *pX Vegfr-1 tk*$^{-/-}$ mice. Synovial hyperplasia, inflammatory infiltrates, pannus formation, and loss of cartilage/bone were reduced by about half in *pX Vegfr-1 tk*$^{-/-}$ mice compared with *pX* wild-type mice ($P = .015$, .011, .007, and .026, respectively) (Figure 2F). Typical histologic findings are shown in Figure 2C-E.

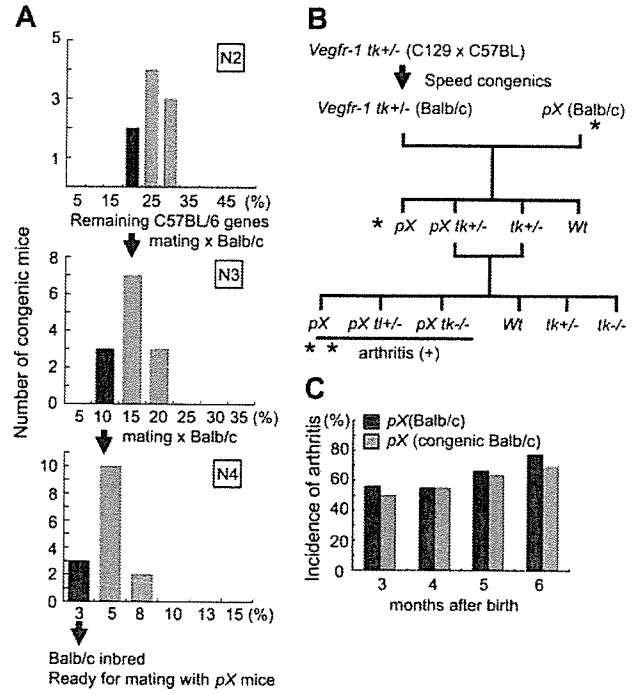

Figure 1. Experimental design and speed congenics used to shorten the period of backcrossing. (A) Percentage of the C57BL/6 polymorphism loci remaining in the backcrossed generation of mice. After 4 generations, a few mice had less than 3% of C57BL/6 background loci. (B) Experimental design for *pX*-induced RA in the *Vegfr-1 tk*$^{-/-}$ background. *Confirmation of the incidence of arthritis in newly prepared BALB/c speed congenic *pX* and original BALB/c *pX* transgenic mice. **The incidence and degree of arthritis in these mice were examined. (C) Comparison of the incidence of arthritis between newly prepared BALB/c speed congenic *pX* transgenic mice and original BALB/c *pX* transgenic mice. No difference was observed during the first 3 to 6 months after birth.

Because VEGFR-1 is considered to be associated with angiogenesis, we examined capillary formation in the pannus of synovial tissue. Capillary densities were about 17% lower in *pX Vegfr-1 tk*$^{-/-}$ mice than *pX* wild-type mice; however, the difference was not significant ($P = .623$) (Figure 3A-C). These results suggest that VEGFR-1 TK–dependent signals contribute to the symptoms of arthritis, including pathological findings, in a gene-dosage–dependent manner.

Production of cytokines by monocytes/macrophages and the function of these cells are important for arthritis

We and others already showed that VEGFR-1 is expressed on monocytes/macrophages[12,13] and that the VEGF-dependent migration of macrophages is suppressed in *Vegfr-1 tk*$^{-/-}$ mice.[17] Therefore, we examined local infiltration and the functions of monocytes/macrophages in these mice. The infiltration of inflammatory cells into arthritic joints was significantly less extensive in *pX Vegfr-1 tk*$^{-/-}$ mice than in *pX* wild-type mice (Figure 2D-F). We also observed using real-time RT-PCR that angiogenic factors and proinflammatory cytokines are up-regulated in their expression in inflammatory joints of *pX* transgenic mice compared with wild-type mice (Figure S2).

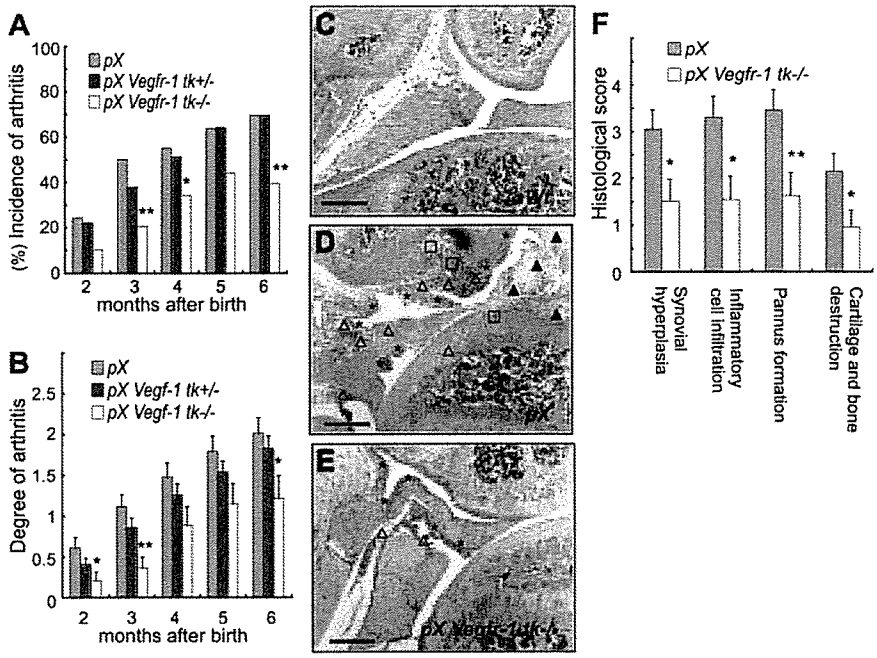

Figure 2. Signals from VEGFR-1 TK contribute to the onset and progression of arthritis. (A) The incidence of arthritis was significantly lower in *pX Vegfr-1 tk*$^{-/-}$ mice than *pX* mice. In addition, the incidence of arthritis in *pX Vegfr-1 tk*$^{+/-}$ heterozygotes was slightly lower in the early stages. (B) Clinical grades of arthritis were reduced depending on the deficiency of the VEGFR-1 TK domain from 2 to 6 months after birth. *pX Vegfr-1 tk*$^{+/-}$ mice showed mild clinical scores between those of *pX* and *pX Vegfr-1 tk*$^{-/-}$ mice. The data (A-B) represent the mean ± SEM obtained from 33 to 122 mice. *$P < .05$ versus *pX*; **$P < .01$ versus *pX*. (C-E) Cross-sections of ankle joints in control and RA mice. Joints of wild-type mice (C) show no remarkable change. Joints of *pX* mice (D) show synovial hyperplasia (*), inflammatory cell infiltration (△), pannus formation (▲), and loss of cartilage and bone (□). These findings are milder in *pX Vegfr-1 tk*$^{-/-}$ mice (E). Sections are taken from average cases in these mice. Scale bars, 200 μm. Images in panels C-E were taken with a Nikon Eclipse TE600 microscope (Nikon, Tokyo, Japan) using AxioVision 3.0 software (Carl Zeiss, Jena, Germany) and a 10×/0.30 NA objective lens, then processed with Photoshop CS (Adobe Systems, San Jose, CA). (F) Histologic scores of the degree of pathology in paws and ankles. Scores of *pX Vegfr-1 tk*$^{-/-}$ mice were about half those of the *pX* mice. The data represent the mean ± SEM. *$P < .05$ versus *pX*; **$P < .01$ versus *pX*.

Secretion of cytokines and phagocytosis are attenuated in *Vegfr-1 tk*$^{-/-}$ macrophages

Saijo et al[39] recently reported that *pX Il-1*$^{-/-}$ mice show a dramatically decreased incidence of arthritis. Because macrophages are an important source of these cytokines, we next focused on the function of macrophages derived from wild-type and *Vegfr-1 tk*–deficient mice. Secretion of IL-6 and VEGF-A was measured in the presence or absence of hVEGF-A. IL-6 was secreted in response to hVEGF-A both in the wild-type and in the *Vegfr-1 tk*$^{-/-}$ mice (Figure 4A). However, much less IL-6 was secreted from *Vegfr-1 tk*$^{-/-}$ macrophages than *Vegfr-1* wild-type cells. In addition, the secretion of IL-6 was partially suppressed with VEGFR inhibitors, SU5416 and KRN633, in the presence of hVEGF-A (Figure 4A).

VEGF-A was secreted from macrophages, and the secretion increased in response to exogenous hVEGF-A (Figure 4B). However, the secretion of VEGF-A from *Vegfr-1 tk*$^{-/-}$ macrophages was about half that in the wild-type mice (Figure 4B).

We examined the mRNA levels of *Il-6* and *Vegf-A* in macrophages in the presence or absence of hVEGF-A by real-time RT-PCR. The expression of both *Il-6* and *Vegf-A* was significantly suppressed in *Vegfr-1 tk*$^{-/-}$ macrophages ($P = .021$ and $< .001$, respectively) (Figure 4C). These results are consistent with the levels of protein determined by ELISA (Figure 4A-B).

Macrophages are multifunctional cells involved in immunologic reactions and phagocytosis. Therefore, we next examined the extent of phagocytosis using macrophages that were induced to differentiate in culture. Wild-type BM-derived and M-CSF–stimulated macrophages efficiently phagocytized both fluorescent dextran and LPS. Surprisingly, however, macrophages from *Vegfr-1 tk*–deficient mice showed significantly less phagocytotic activity (Figure 4D).

Therefore, in addition to the suppression of VEGF-A–dependent migration, *Vegfr-1 tk*-deficient macrophages were dysfunctional in the secretion of IL-6 and VEGF-A as well as phagocytosis under these experimental conditions.

VEGFR TK inhibitor, KRN951, suppressed the progression of arthritis

To confirm the therapeutic effect of VEGFR kinase inhibitors on arthritis, we administered such an inhibitor, KRN951, to mice with *pX*-induced chronic arthritis and collagen-antibody–induced acute arthritis. We treated the mice with KRN951 for 5 straight days (oral, 20 mg/kg/d) a week from 8 to 26 weeks of age (Figure 5A). Administration of KRN951 reduced the progression of arthritis compared with the control ($P < .041$ from 18 weeks to 26 weeks) (Figure 5B). Histologic abnormalities in the treated group decreased 11% to 25% compared with the control (statistically not significant) (Figure 5C). In our preliminary experiments, a dose of KRN951 (1.0 mg/kg body weight) lower than those used in this experiment strongly suppressed the growth of several solid tumors in vivo in mice, suggesting that the dose of KRN951 used here

Figure 3. No significant difference was observed in newly formed vessel densities in the hyperplastic synovia and pannus between *pX* mice and *pX Vegfr-1 tk*$^{-/-}$ mice. (A-B) Staining for VWF in the newly formed capillary vessels in the hyperplastic synovia and pannus. Scale bars, 50 μm. Images were taken with a Nikon Eclipse TE600 microscope, using AxioVision 3.0 software and a 40×/0.75 NA objective lens, then processed with Photoshop CS. (C) Vascular densities in the hyperplastic synovia are slightly lower in *pX Vegfr-1 tk*$^{-/-}$ mice than in *pX* mice ($P = .623$). The data represent the mean ± SEM.

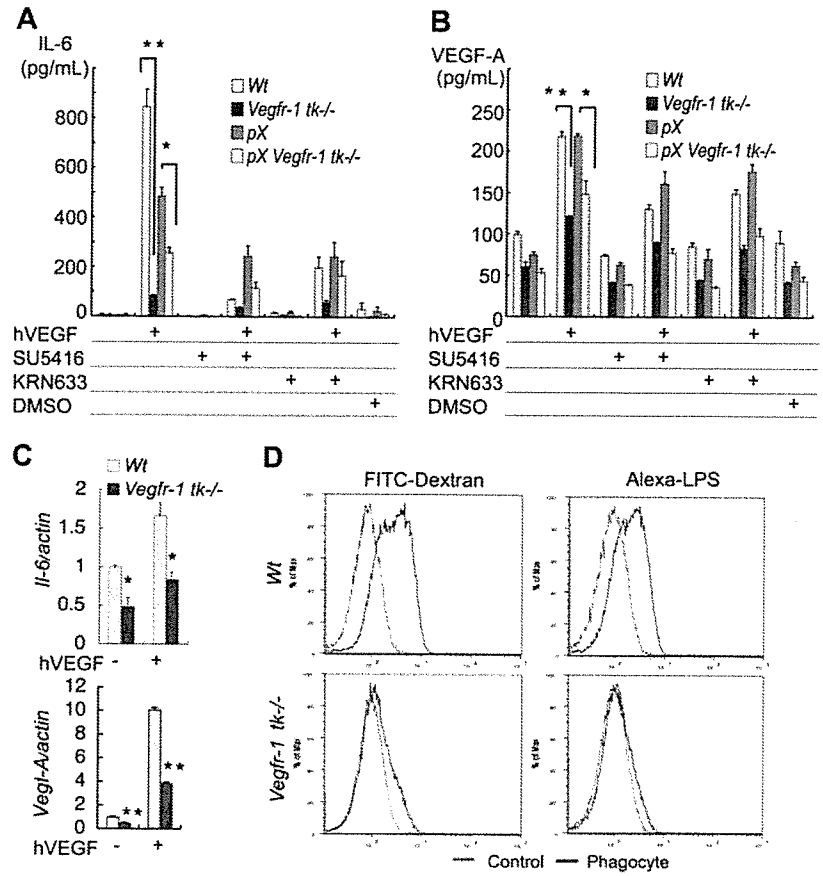

Figure 4. Cytokine secretion and phagocytosis are attenuated in the macrophages in *Vegfr-1 tk*$^{-/-}$ mice. (A-B) Mouse peritoneal macrophages were stimulated with hVEGF-A (100 ng/mL), and then levels of cytokines (IL-6 and VEGF-A) secreted into the medium were measured by ELISA after a 48-hour incubation. (A) IL-6 was secreted in response to hVEGF-A, and this secretion was partially suppressed by VEGFR inhibitors, SU5416 and KRN633. Secretion of IL-6 from *Vegfr-1 tk*$^{-/-}$ macrophages was low compared with that from the wild-type macrophages. (B) Mouse VEGF-A (mVEGF-A) was secreted from macrophages in the absence of hVEGF-A, and the secretion increased on stimulation with exogenous hVEGF-A. The secretion of mVEGF-A was partially suppressed by VEGFR inhibitors. The secretion from *Vegfr-1 tk*$^{-/-}$ macrophages was about half that from wild-type macrophages. Results represent the mean ± SEM from 2 to 3 experiments. (C) The mRNA expression of *Il-6* and *Vegf-A* on treatment with hVEGF-A was examined by real-time RT-PCR analysis. *Il-6* is weakly expressed in *Vegfr-1 tk*$^{-/-}$ macrophages. *Vegf-A* expression in *Vegfr-1 tk*$^{-/-}$ macrophages is about half that in the wild-type. (D) Macrophages derived from wild-type BM cells in cultures phagocytized dextran and LPS (upper row). On the other hand, macrophages from *Vegfr-1 tk*$^{-/-}$ BM did not show strong phagocytosis (lower row). Results are representative of at least 3 independent experiments. The data represent the mean ± SEM. $^*P < .05$, $^{**}P < .01$; wild-type versus *Vegfr-1 tk*$^{-/-}$ macrophages.

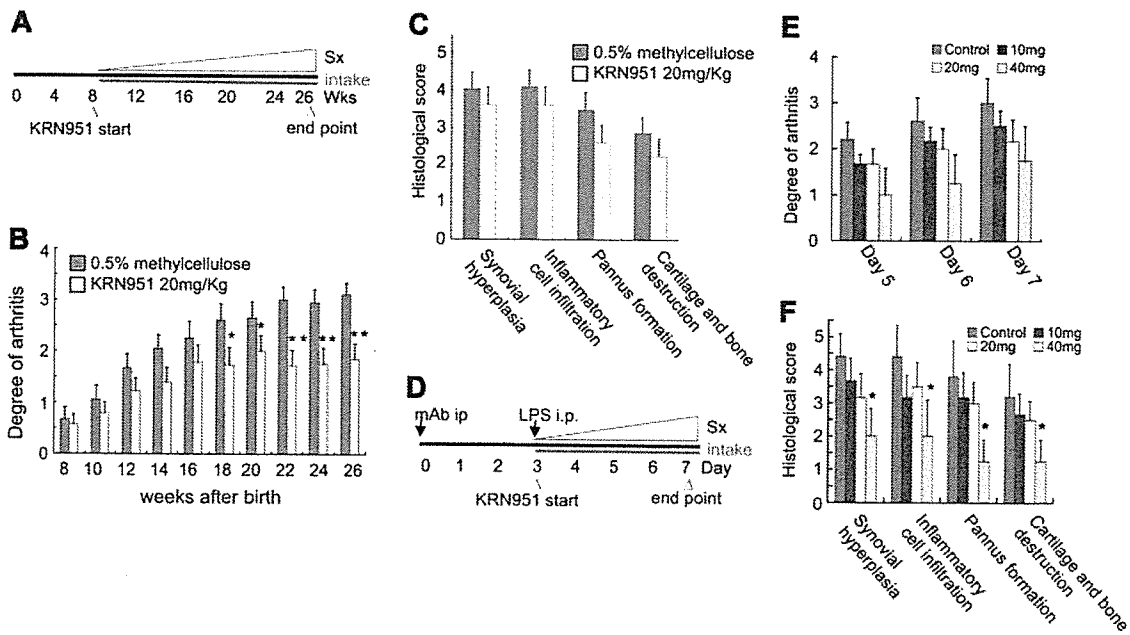

Figure 5. A VEGFR TK inhibitor, KRN951, suppressed the progression of *pX*-induced chronic and collagen-antibody–induced acute arthritis. (A) Experimental design for the treatment of mice with *pX*-induced chronic arthritis with a VEGFR inhibitor, KRN951. The VEGFR inhibitor was orally administered from 8 to 26 weeks of age (5 d/wk). (B) Clinical grades of arthritis gradually increased with age. The KRN951-administered group showed a reduction in the progression of arthritis compared with the untreated group. The data represent the mean ± SEM. $^*P < .05$, $^{**}P < .01$; KRN951-treated group versus control. (C) The scores of histologic findings in the treated group were also decreased (statistically not significant). (D) Experimental design for the treatment of mice with collagen-antibody–induced acute arthritis. Anticollagen-antibody was injected into the peritoneum of mice, followed by a peritoneal injection of LPS after 3 days. The administration of KRN951 started at day 3 and ended at day 7. (E-F) Clinical grade and histologic score of acute arthritis decreased in a KRN951 dose–dependent manner. The data represent the mean ± SEM. $^*P < .05$; 40 mg/kg/d versus control. Sx indicates symptom.

could block the TK of VEGFR1 and VEGFR2 in vivo (K.N. and M.S., unpublished data, April 2006).

The administration of KRN951 in the acute model also reduced the progression of the symptoms of arthritis in a dose-dependent manner ($P = .142$ to $.227$ on day 5 to day 7. All values are 40 mg/kg/d versus control) (Figure 5E). KRN951 is a pan-VEGFR inhibitor; however, the arthritic symptoms and histologic abnormalities with KRN951 were as mild as those of *pX Vegfr-1 tk*–deficient mice. Taken together, these results suggest that VEGFR TKs, particularly VEGFR-1, contribute to the progression of arthritis.

VEGFR-1 is closely associated with the proliferation/differentiation of hematopoietic cells but not the number of BM hematopoietic stem cells

Another hallmark of hematopoietic activity is the capacity for colonies to form BMMNCs in vitro.[40] The colony-forming ability of *Vegfr-1* $tk^{-/-}$ BMMNCs was reduced to about 70% of that of wild-type BMMNCs ($P = .013$), and all the progenitors including erythroid colonies, myeloid colonies, and more immature mixed colonies were equally affected ($P = .002$, $.091$, and $.021$, respectively) (Figure 6A-B).

These results suggest at least 2 possibilities: a decrease in the activity of BM hematopoietic stem cells (HSCs) or a decrease in the number of HSCs in *Vegfr-1* $tk^{-/-}$ BM. To distinguish between these possibilities, we examined the number of HSCs by FACS analysis. Numbers of Sca-1^+ and $CD34^+$ cells corresponding to HSCs among BMMNCs were almost the same between wild-type and *Vegfr-1* $tk^{-/-}$ mice (Figure 6C). Therefore, a deficiency of VEGFR-1 signaling may reduce the proliferation of HSCs but not the number of these cells in BM.

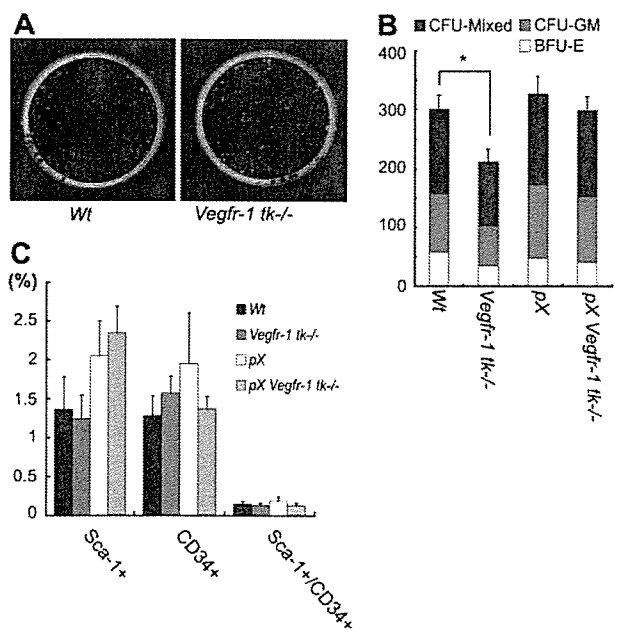

Figure 6. VEGFR-1 is associated with the proliferation of hematopoietic cells but not the number of BM HSCs. (A-B) The number of colony-forming units (CFU) in *Vegfr-1* $tk^{-/-}$ was decreased in all progenitor cells (BFU-E, CFU-GM, CFU-mixed) compared with that in wild-type mice ($P = .013$) (A). Each progenitor cell also showed a decrease in the number of colonies ($P = .002$ in BFU-E, $.091$ in CFU-GM, and $.021$ in CFU-mixed). Data represent the mean ± SEM for 3 mice. $^*P < .05$; wild-type BM versus *Vegfr-1* $tk^{-/-}$ BM (B). (C) The number of HSCs (Sca-1^+ and $CD34^+$ cells) in BM was not influenced by *Vegfr-1 tk* deficiency. Percentages of HSCs among BMMNCs were analyzed by flow cytometer. Results represent the mean ± SEM for 3 mice.

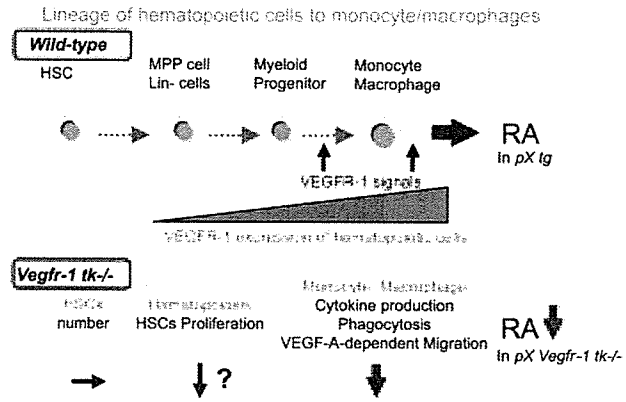

Figure 7. VEGFR-1 TK signaling is involved in arthritis by modulating hematopoiesis and promoting the differentiation of monocytes/macrophages. A schematic model of the VEGFR-1 TK signals associated with arthritis. (Top) Immature monocytes/macrophages derived from BM hematopoietic cells differentiate and migrate into the circulation. VEGFR-1 is expressed in monocyte/macrophage lineages. VEGFR-1 signals mobilize inflammatory cells to the peripheral tissues and RA joints and stimulate secretion of inflammatory cytokines to promote RA. (Bottom) VEGFR-1 signal–deficient macrophages show suppressed cytokine secretion, phagocytosis, and VEGF-dependent migration, resulting in a decrease in RA.

Discussion

In this study, we have shown that VEGFR-1 TK signals play a significant role in the progression of RA in murine models of both chronic and acute arthritis. Furthermore, the involvement of VEGFR-1 signals is considered to be gene-dosage dependent because the clinical and histologic scores of RA in *Vegfr-1* $tk^{+/-}$ heterozygous *pX* mice were between those of wild-type *pX* and *Vegfr-1* $tk^{-/-}$ mice. Several functions of macrophages such as the secretion of IL-6 and VEGF-A, phagocytosis, and VEGF-A–dependent migration were clearly suppressed in *Vegfr-1* $tk^{-/-}$ mice. In addition, the proliferation of HSCs decreased about 30% in the in vitro assay in these mice. These results suggest that the kinase activity of VEGFR-1 is important in a variety of steps during the progression of pathological inflammatory diseases such as RA (Figure 7).

Our results raise the question of which receptor for VEGFs, VEGFR-1 or VEGFR-2, is tightly linked to RA. The TK of VEGFR-2 appears to be essential for the maintenance of blood vessel networks in adulthood[4,15,20,41-44]; thus, *Vegfr-2* tk^- mice, similar to the *Vegfr-1* $tk^{-/-}$ mice in this study, are not available. However, the suppressive effect of *Vegfr-1 tk* deficiency on the RA model and that of the treatment with the pan-VEGFR kinase inhibitor KRN951 were similar (Figures 2 and 5A), suggesting that VEGFR-1 signaling is more strongly related to the progression of RA than VEGFR-2 signaling. In addition, the amount of newly formed capillary vessels in the pannus did not differ significantly between *pX Vegfr-1* $tk^{+/+}$ and *pX Vegfr-1* $tk^{-/-}$ mice. These results imply that inflammatory responses are more closely associated with VEGFR-1 than VEGFR-2. Consistent with these findings, Luttun et al[22] found that, using blocking antibodies against mouse VEGFR-1 or VEGFR-2, treatment with anti–VEGFR-1 Ab more efficiently suppressed an adjuvant-induced inflammatory arthritis than did treatment with anti–VEGFR-2 Ab. Furthermore, De Bandt et al[45] recently reported that VEGFR-1 is involved in a model of chronic arthritis in which the KRN/NOD ($\alpha v\beta 6$ T-cell receptor [TCR] transgene)/nonobese diabetic) mice were used for the induction of inflammation. Their model system is different from ours; therefore, results obtained with several independent animal

models of arthritis clearly support the importance of VEGFR-1 in this disease.

It is of interest that the suppression of chronic RA in the *pX* mice is dependent on the dosage of the *Vegfr-1 tk* gene to some extent. We and others previously showed that the kinase activity of VEGFR-1 is one order of magnitude lower than that of VEGFR-2.[46,47] These results suggest that the limiting step in the VEGFR-1 signaling pathway to promote RA is not the amount of ligand such as VEGF-A but the amount of VEGFR-1 itself. They may also support the idea that VEGFR-1 TK activity is a good pharmaceutical target for control of chronic RA.

Several groups including ours have shown that VEGFR-1 is well expressed in monocytes/macrophages at both the mRNA and protein levels[12,13] and that VEGFR-1 is important for the VEGF-A–dependent migration of these cells.[11,17] Therefore, it is reasonable that the infiltration of inflammatory cells was significantly less extensive in *Vegfr-1 tk*–deficient *pX* mice than wild-type *pX* mice (Figure 2D-F). Surprisingly, the blocking of the VEGFR-1 signals via deletion of its TK domain clearly suppressed the additional functions of these macrophages such as the secretion of IL-6 and VEGF-A stimulated by hVEGF and the phagocytotic reaction to dextran and LPS. The latter phenomenon is particularly interesting because the process of phagocytosis was thought to be a broad/nonspecific reaction against exogenous materials entering the body. On the other hand, macrophages obtained directly from the abdominal cavity of *Vegfr-1* $tk^{-/-}$ mice exhibit phagocytotic activity similar to that of their wild-type counterparts (data not shown). It should be clarified whether the process of phagocytosis is directly dependent on the signaling of VEGFR-1 or whether the maturation of macrophages to obtain phagocytotic activity is delayed under VEGFR-1 signal–deficient conditions.

A VEGFR TK inhibitor, KRN951, also had suppressive effects on the *pX*-induced RA mouse model (Figure 5). Although the histologic scores indicated in Figure 5C are not statistically significant, the differences in the degree of arthritis more than 18 weeks after birth are significant (Figure 5B). Interestingly, the changes in RA observed between *pX* and *pX/Vegfr-1* $tk^{-/-}$ mice (Figure 2F) were more significant than those in Figure 5C. To explain these results, we suggest that *Vegfr-1 tk*–deficient mice lost all signaling from VEGFR-1, whereas the treatment of mice with a VEGFR kinase inhibitor such as KRN951 is usually incomplete in blocking the kinase activity.

Our results suggest that VEGFR-1 has an effect on the proliferation of HSCs in CFU-B. All of the multilineage colonies (ie, BFU-E, CFU-GM, and CFU-mixed) are suppressed in *Vegfr-1 tk*–deficient BM HSCs. However, the number of HSCs positive for Sca-1 and CD34 was not so different from that in wild-type mice (Figure 6C). There are several potential explanations for these results: (1) *Vegfr-1 tk* deficiency causes a functional defect in macrophages in BM, which, in turn, indirectly causes an abnormality among HSCs; (2) VEGFR-1 expressed on the HSCs has a direct effect on cell signaling, and the lack of this signaling results in an abnormal phenotype; or (3) both mechanisms synergistically affect the function of HSCs. Although the number of these cells is small, a quantitative analysis appears to be necessary to clarify these possibilities.

RA is a chronic disease of late onset, and multiple pathways of inflammation and immune systems appear to be involved. A recent study indicated that the artificial blocking of TNF-α and IL-6 receptor by neutralizing antibodies significantly (but not completely) suppressed clinical as well as histologic scores in patients.[48] VEGFR-1 signaling is involved in multiple functions of macrophages as a part of the functions of HSCs. Because these functions are at least partly independent of the TNF-α–IL-6 pathway, it appears reasonable that, in addition to inhibition of the TNF-α–IL-6 pathway, suppression of VEGFR-1 signaling by either a specific antibody or a small inhibitor molecule may significantly improve the condition of RA patients.

Acknowledgments

We thank Dr S. Saijo (Division of Cell Biology) and Dr K. Hattori and Dr Y Morita (Division of Stem Cell Therapy, Center for Experimental Medicine, Institute of Medical Science, University of Tokyo) for technical assistance and helpful discussions.

References

1. Mustonen T, Alitalo K. Endothelial receptor tyrosine kinases involved in angiogenesis. J Cell Biol. 1995;129:895-898.
2. Ferrara N, Davis-Smyth T. The biology of vascular endothelial growth factor. Endocr Rev. 1997; 18:4-25.
3. Risau W. Mechanisms of angiogenesis. Nature. 1997;386:671-674.
4. Shibuya M. Structure and function of VEGF/VEGF-receptor system involved in angiogenesis. Cell Struct Funct. 2001;26:25-35.
5. Shibuya M, Yamaguchi S, Yamane A, et al. Nucleotide sequence and expression of a novel human receptor-type tyrosine kinase gene (flt) closely related to the fms family. Oncogene. 1990;5:519-524.
6. Kondo K, Hiratsuka S, Subbalakshmi E, Matsushime H, Shibuya M. Genomic organization of the flt-1 gene encoding for vascular endothelial growth factor (VEGF) receptor-1 suggests an intimate evolutionary relationship between the 7-Ig and the 5-Ig tyrosine kinase receptors. Gene. 1998;208:297-305.
7. Jakeman LB, Winer J, Bennett GL, Altar CA, Ferrara N. Binding sites for vascular endothelial growth factor are localized on endothelial cells in adult rat tissues. J Clin Invest. 1992;89:244-253.
8. Eichmann A, Marcelle C, Breant C, Le Douarin NM. Two molecules related to the VEGF receptor are expressed in early endothelial cells during avian embryonic development. Mech Dev. 1993; 42:33-48.
9. Kaipainen A, Korhonen J, Pajusola K, et al. The related FLT4, FLT1, and KDR receptor tyrosine kinases show distinct expression patterns in human fetal endothelial cells. J Exp Med. 1993;178: 2077-2088.
10. Yamane A, Seetharam L, Yamaguchi S, et al. A new communication system between hepatocytes and sinusoidal endothelial cells in liver through vascular endothelial growth factor and Flt tyrosine kinase receptor family (Flt-1 and KDR/Flk-1). Oncogene. 1994;9:2683-2690.
11. Barleon B, Sozzani S, Zhou D, Weich HA, Mantovani A, Marme D. Migration of human monocytes in response to vascular endothelial growth factor (VEGF) is mediated via the VEGF receptor flt-1. Blood. 1996;87:3336-3343.
12. Clauss M, Weich H, Breier G, et al. The vascular endothelial growth factor receptor Flt-1 mediates biological activities: implications for a functional role of placenta growth factor in monocyte activation and chemotaxis. J Biol Chem. 1996;271: 17629-17634.
13. Sawano A, Iwai S, Sakurai Y, et al. Flt-1, vascular endothelial growth factor receptor 1, is a novel cell surface marker for the lineage of monocyte-macrophages in humans. Blood. 2001;97:785-791.
14. Shibuya M. Structure and dual function of vascular endothelial growth factor receptor-1 (Flt-1). Int J Biochem Cell Biol. 2001;33:409-420.
15. Shalaby F, Rossant J, Yamaguchi TP, et al. Failure of blood-island formation and vasculogenesis in Flk-1-deficient mice. Nature. 1995;376:62-66.
16. Fong GH, Rossant J, Gertsenstein M, Breitman ML. Role of the Flt-1 receptor tyrosine kinase in regulating the assembly of vascular endothelium. Nature. 1995;376:66-70.
17. Hiratsuka S, Minowa O, Kuno J, Noda T, Shibuya M. Flt-1 lacking the tyrosine kinase domain is sufficient for normal development and angiogenesis in mice. Proc Natl Acad Sci U S A. 1998;95:9349-9354.
18. Luo JC, Toyoda M, Shibuya M. Differential inhibition of fluid accumulation and tumor growth in two mouse ascites tumors by an antivascular endothelial growth factor/permeability factor neutralizing antibody. Cancer Res. 1998;58: 2594-2600.
19. Autiero M, Luttun A, Tjwa M, Carmeliet P. Placental growth factor and its receptor, vascular endothelial growth factor receptor-1: novel targets for stimulation of ischemic tissue revascularization

and inhibition of angiogenic and inflammatory disorders. J Thromb Haemost. 2003;1:1356-1370.

20. Ferrara N, Gerber HP, LeCouter J. The biology of VEGF and its receptors. Nat Med. 2003;9:669-676.
21. Carmeliet P, Moons L, Luttun A, et al. Synergism between vascular endothelial growth factor and placental growth factor contributes to angiogenesis and plasma extravasation in pathological conditions. Nat Med. 2001;7:575-583.
22. Luttun A, Tjwa M, Moons L, et al. Revascularization of ischemic tissues by PlGF treatment, and inhibition of tumor angiogenesis, arthritis and atherosclerosis by anti-Flt1. Nat Med. 2002;8:831-840.
23. Hiratsuka S, Maru Y, Okada A, Seiki M, Noda T, Shibuya M. Involvement of Flt-1 tyrosine kinase (vascular endothelial growth factor receptor-1) in pathological angiogenesis. Cancer Res. 2001;61:1207-1213.
24. Hiratsuka S, Nakamura K, Iwai S, et al. MMP9 induction by vascular endothelial growth factor receptor-1 is involved in lung-specific metastasis. Cancer Cell. 2002;2:289-300.
25. Hattori K, Heissig B, Wu Y, et al. Placental growth factor reconstitutes hematopoiesis by recruiting VEGFR1(+) stem cells from bone-marrow microenvironment. Nat Med. 2002;8:841-849.
26. Clague RB, Shaw MJ, Holt PJ. Incidence of serum antibodies to native type I and type II collagens in patients with inflammatory arthritis. Ann Rheum Dis. 1980;39:201-206.
27. Firestein GS. Mechanisms of tissue destruction and cellular activation in rheumatoid arthritis. Curr Opin Rheumatol. 1992;4:348-354.
28. Firestein GS, Zvaifler NJ. Rheumatoid arthritis: a disease of disorderd immunity. In: Gallin JI, Goldstein IM, Synderman R, eds. Inflammation: Basic Principles and Clinical Correlations. New York, NY: Raven Press; 1992:959-975.
29. Fava RA, Olsen NJ, Spencer-Green G, et al. Vascular permeability factor/endothelial growth factor (VPF/VEGF): accumulation and expression in human synovial fluids and rheumatoid synovial tissue. J Exp Med. 1994;180:341-346.
30. Koch AE, Harlow LA, Haines GK, et al. Vascular endothelial growth factor: a cytokine modulating endothelial function in rheumatoid arthritis. J Immunol. 1994;152:4149-4156.
31. Lee DM, Weinblatt ME. Rheumatoid arthritis. Lancet. 2001;358:903-911.
32. Iwakura Y, Tosu M, Yoshida E, et al. Induction of inflammatory arthropathy resembling rheumatoid arthritis in mice transgenic for HTLV-I. Science. 1991;253:1026-1028.
33. Iwakura Y, Saijo S, Kioka Y, et al. Autoimmunity induction by human T cell leukemia virus type 1 in transgenic mice that develop chronic inflammatory arthropathy resembling rheumatoid arthritis in humans. J Immunol. 1995;155:1588-1598.
34. Iwakura Y, Itagaki K, Ishitsuka C, et al. The development of autoimmune inflammatory arthropathy in mice transgenic for the human T cell leukemia virus type-1 env-pX region is not dependent on H-2 haplotypes and modified by the expression levels of Fas antigen. J Immunol. 1998;161:6592-6598.
35. Habu K, Nakayama-Yamada J, Asano M, et al. The human T cell leukemia virus type I-tax gene is responsible for the development of both inflammatory polyarthropathy resembling rheumatoid arthritis and noninflammatory ankylotic arthropathy in transgenic mice. J Immunol. 1999;162:2956-2963.
36. The Jackson Laboratory. Mouse Genome Informatics. Available at: http://www.informatics.jax.org. Accessed July 18, 2006.
37. Fong TA, Shawver LK, Sun L, et al. SU5416 is a potent and selective inhibitor of the vascular endothelial growth factor receptor (Flk-1/KDR) that inhibits tyrosine kinase catalysis, tumor vascularization, and growth of multiple tumor types. Cancer Res. 1999;59:99-106.
38. Nakamura K, Yamamoto A, Kamishohara M, et al. KRN633: a selective inhibitor of vascular endothelial growth factor receptor-2 tyrosine kinase that suppresses tumor angiogenesis and growth. Mol Cancer Ther. 2004;3:1639-1649.
39. Saijo S, Asano M, Horai R, Yamamoto H, Iwakura Y. Suppression of autoimmune arthritis in interleukin-1-deficient mice in which T cell activation is impaired due to low levels of CD40 ligand and OX40 expression on T cells. Arthritis Rheum. 2002;46:533-544.
40. Vos O, Ploemacher RE. Developments in modern hematology. Boll Soc Ital Biol Sper. 1991;67:435-458.
41. Kasahara Y, Tuder RM, Taraseviciene-Stewart L, et al. Inhibition of VEGF receptors causes lung cell apoptosis and emphysema. J Clin Invest. 2000;106:1311-1319.
42. Eremina V, Sood M, Haigh J, et al. Glomerular-specific alterations of VEGF-A expression lead to distinct congenital and acquired renal diseases. J Clin Invest. 2003;111:707-716.
43. Gerber HP, McMurtrey A, Kowalski J, et al. Vascular endothelial growth factor regulates endothelial cell survival through the phosphatidylinositol 3′-kinase/Akt signal transduction pathway: requirement for Flk-1/KDR activation. J Biol Chem. 1998;273:30336-30343.
44. Takahashi T, Ueno H, Shibuya M. VEGF activates protein kinase C-dependent, but Ras-independent Raf-MEK-MAP kinase pathway for DNA synthesis in primary endothelial cells. Oncogene. 1999;18:2221-2230.
45. De Bandt M, Ben Mahdi MH, Ollivier V, et al. Blockade of vascular endothelial growth factor receptor I (VEGF-RI), but not VEGF-RII, suppresses joint destruction in the K/BxN model of rheumatoid arthritis. J Immunol. 2003;171:4853-4859.
46. Seetharam L, Gotoh N, Maru Y, Neufeld G, Yamaguchi S, Shibuya M. A unique signal transduction from FLT tyrosine kinase, a receptor for vascular endothelial growth factor VEGF. Oncogene. 1995;10:135-147.
47. Sawano A, Takahashi T, Yamaguchi S, Aonuma M, Shibuya M. Flt-1 but not KDR/Flk-1 tyrosine kinase is a receptor for placenta growth factor, which is related to vascular endothelial growth factor. Cell Growth Differ. 1996;7:213-221.
48. McInnes IB, Gracie JA. Targeting cytokines beyond tumor necrosis factor-alpha and interleukin-1 in rheumatoid arthritis. Curr Rheumatol Rep. 2004;6:336-342.

Science
AAAS

The Muscle Protein Dok-7 Is Essential for Neuromuscular Synaptogenesis

Kumiko Okada, *et al.*

Science **312**, 1802 (2006);
DOI: 10.1126/science.1127142

Science (print ISSN 0036-8075; online ISSN 1095-9203) is published weekly, except the last week in December, by the American Association for the Advancement of Science, 1200 New York Avenue NW, Washington, DC 20005.

changes at or near promoters, whereas TopoI inhibitors caused transcription complexes to stall in the midst of transcription units (*34*).

Collectively, our data reveal that a transient dsDNA break occurs at multiple regulated transcription units. This raises questions regarding the interplay between molecular machineries that are involved in the repair of dsDNA breaks and the activation of the gene transcription.

References and Notes

1. C. K. Glass, M. G. Rosenfeld, *Genes Dev.* **14**, 121 (2000).
2. B. M. Spiegelman, R. Heinrich, *Cell* **119**, 157 (2004).
3. V. Perissi, M. G. Rosenfeld, *Nat. Rev. Mol. Cell Biol.* **6**, 542 (2005).
4. A. Tulin, D. Stewart, A. C. Spradling, *Genes Dev.* **16**, 2108 (2002).
5. R. Pavri *et al.*, *Mol. Cell* **18**, 83 (2005).
6. M. Y. Kim, S. Mauro, N. Gevry, J. T. Lis, W. L. Kraus, *Cell* **119**, 803 (2004).
7. B. G. Ju *et al.*, *Cell* **119**, 815 (2004).
8. M. Malanga, F. R. Althaus, *Biochem. Cell Biol.* **83**, 354 (2005).
9. S. Burma, D. J. Chen, *DNA Repair* **3**, 909 (2004).
10. J. M. Jeltsch *et al.*, *Nucleic Acids Res.* **15**, 1401 (1987).
11. J. C. Wang, *Nat. Rev. Mol. Cell Biol.* **3**, 430 (2002).
12. A. Dvir, S. R. Peterson, M. W. Knuth, H. Lu, W. S. Dynan, *Proc. Natl. Acad. Sci. U.S.A.* **89**, 11920 (1992).
13. T. Chibazakura *et al.*, *Eur. J. Biochem.* **247**, 1166 (1997).
14. C. A. Sartorius, G. S. Takimoto, J. K. Richer, L. Tung, K. B. Horwitz, *J. Mol. Endocrinol.* **24**, 165 (2000).
15. G. L. Mayeur *et al.*, *J. Biol. Chem.* **280**, 10827 (2005).
16. C. Leontiou, J. H. Lakey, R. Lightowlers, R. M. Turnbull, C. A. Austin, *Mol. Pharmacol.* **69**, 130 (2006).
17. R. Metivier *et al.*, *Cell* **115**, 751 (2003).
18. L. Ko, G. R. Cardona, W. W. Chin, *Proc. Natl. Acad. Sci. U.S.A.* **97**, 6212 (2000).
19. S. K. Lee *et al.*, *Mol. Endocrinol.* **14**, 915 (2000).
20. J. Torchia *et al.*, *Nature* **387**, 677 (1997).
21. M. Binaschi, R. Farinosi, M. E. Borgnetto, G. Capranico, *Cancer Res.* **60**, 3770 (2000).
22. M. N. Cervellera, A. Sala, *J. Biol. Chem.* **275**, 10692 (2000).
23. P. O. Hassa, M. Covic, S. Hasan, R. Imhof, M. O. Hottiger, *J. Biol. Chem.* **276**, 45588 (2001).
24. C. Le Page, J. Sanceau, J. C. Drapier, J. Wietzerbin, *Biochem. Biophys. Res. Commun.* **243**, 451 (1998).
25. A. J. Butler, C. P. Ordahl, *Mol. Cell. Biol.* **19**, 296 (1999).
26. M. Ku, S. Stewart, A. Hata, *Biochem. Biophys. Res. Commun.* **311**, 702 (2003).
27. F. R. Althaus *et al.*, *Mol. Cell. Biochem.* **138**, 53 (1994).
28. D. T. Brown, *Biochem. Cell Biol.* **81**, 221 (2003).
29. J. O. Thomas, *Biochem. Soc. Trans.* **29**, 395 (2001).
30. M. F. Ruh, J. C. Chrivia, L. K. Cox, T. S. Ruh, *Mol. Cell. Endocrinol.* **214**, 71 (2004).
31. D. Das, R. C. Peterson, W. M. Scovell, *Mol. Endocrinol.* **18**, 2616 (2004).
32. A. M. Nunez, M. Berry, J. L. Imler, P. Chambon, *EMBO J.* **8**, 823 (1989).
33. T. Barkhem, L. A. Haldosen, J. A. Gustafsson, S. Nilsson, *Mol. Pharmacol.* **61**, 1273 (2002).
34. I. Collins, A. Weber, D. Levens, *Mol. Cell. Biol.* **21**, 8437 (2001).

35. We thank C. Nelson and K. Ohgi for their assistance; S. Ogawa and J. Puc for reagents; and X. Zhu and T. Wang for discussions and advice. We also thank J. Hightower and M. Fisher for assistance in figure and manuscript preparation and M. Gonzalez (Santa Cruz Biotechnology) for advice on reagents. M.G.R. is an investigator with the Howard Hughes Medical Institute and B.J. is supported by the U.S. Army Medical Research and Materiel Command (grant DAMD17-01-1-0184). These studies are supported by NIH and National Cancer Institute grants to M.G.R. and C.K.G.

Supporting Online Material

www.sciencemag.org/cgi/content/full/312/5781/1798/DC1
Materials and Methods
Figs. S1 to S5
References

9 March 2006; accepted 4 May 2006
10.1126/science.1127196

The Muscle Protein Dok-7 Is Essential for Neuromuscular Synaptogenesis

Kumiko Okada,[1]* Akane Inoue,[1]* Momoko Okada,[1] Yoji Murata,[1] Shigeru Kakuta,[3] Takafumi Jigami,[4] Sachiko Kubo,[3] Hirokazu Shiraishi,[5] Katsumi Eguchi,[5] Masakatsu Motomura,[5] Tetsu Akiyama,[4] Yoichiro Iwakura,[3] Osamu Higuchi,[1]† Yuji Yamanashi[1,2]†

The formation of the neuromuscular synapse requires muscle-specific receptor kinase (MuSK) to orchestrate postsynaptic differentiation, including the clustering of receptors for the neurotransmitter acetylcholine. Upon innervation, neural agrin activates MuSK to establish the postsynaptic apparatus, although agrin-independent formation of neuromuscular synapses can also occur experimentally in the absence of neurotransmission. Dok-7, a MuSK-interacting cytoplasmic protein, is essential for MuSK activation in cultured myotubes; in particular, the Dok-7 phosphotyrosine-binding domain and its target in MuSK are indispensable. Mice lacking Dok-7 formed neither acetylcholine receptor clusters nor neuromuscular synapses. Thus, Dok-7 is essential for neuromuscular synaptogenesis through its interaction with MuSK.

Skeletal muscle is controlled by motor neurons, which contact the muscle at the neuromuscular junction, a synapse that uses the neurotransmitter acetylcholine (*1*, *2*). To achieve sufficient sensitivity to the neurotransmitter, acetylcholine receptors (AChRs) on the muscle must be densely clustered on the postsynaptic side of the neuromuscular junction (*1*, *2*). Failure of AChR clustering is associated with disorders in neuromuscular transmission, including congenital myasthenic syndrome and myasthenia gravis (*3*, *4*). The presynaptic motor-nerve terminal secretes the glycoprotein agrin to activate postsynaptic MuSK (*5*). This agrin-dependent activation of MuSK is essential to establish the postsynaptic apparatus, including the clustering of AChRs, via the AChR-associated protein Rapsyn (*6*–*8*). Nevertheless, before innervation, MuSK-dependent AChR clusters can form at the endplate area of myotubes, suggesting a mechanism of postsynaptic specialization that is independent of agrin and innervation (*9*–*11*). Furthermore, neuromuscular synapses can form independently of agrin in mice that lack acetylcholine, which appears to antagonize postsynaptic differentiation (*12*, *13*). Thus, in addition to agrin, there may be another element that can achieve MuSK activation and trigger postsynaptic specializations at the neuromuscular junction. MuSK contains a phosphotyrosine-binding domain (PTB domain) target motif Asn-Pro-X-Tyr encompassing Tyr^{553} in the juxtamembrane region, which is essential for proper functioning in vivo (*14*). The binding partner for this motif has remained elusive.

By searching databases, including GenBank, the European Molecular Biology Laboratory, and the DNA Data Bank of Japan, for a previously unidentified member of the Dok-family of proteins, each of which has a PTB domain, we identified Dok-7 and cloned human cDNA encoding 504 amino acids. Like other members, Dok-7 has pleckstrin-homology (PH) and PTB domains in the N-terminal portion and Src homology 2 (SH2) domain target motifs in the C-terminal region (fig. S1) (*15*–*17*). Cloning of mouse (*Mus musculus*) and puffer fish (*Takifugu rubripes*) Dok-7 cDNA revealed a highly conserved structure (fig. S2). Like agrin and MuSK, no ortholog was found in invertebrates such as the fruit fly (*Drosophila melanogaster*) and nematode (*Caenorhabditis elegans*). Northern blot analysis of human tissues showed that Dok-7 mRNA is preferentially expressed in skeletal muscle and in the heart (fig. S3A), and immunoblot analysis identified a 55-kD Dok-7 protein in the thigh muscle, diaphragm, and heart but not in the liver or spleen (fig. S3B). Furthermore, immunostaining of mouse skeletal muscles, including the sternocleidomas-

[1]Department of Cell Regulation, Medical Research Institute, [2]School of Biomedical Science, Tokyo Medical and Dental University, Tokyo 113–8510, Japan. [3]Center for Experimental Medicine, Institute of Medical Science, University of Tokyo, Tokyo 108–8639, Japan. [4]Laboratory of Molecular and Genetic Information, Institute of Molecular and Cellular Biosciences, University of Tokyo, Tokyo 113–0032, Japan. [5]The First Department of Internal Medicine, Graduate School of Biomedical Sciences, Nagasaki University, Nagasaki 852–8501, Japan.

*These authors contributed equally to this work.
†To whom correspondence should be addressed. E-mail: yamanashi.creg@mri.tmd.ac.jp (Y.Y.); higuchi.creg@mri.tmd.ac.jp (O.H.)

toid, extensor digitorum longus, and gastrocnemius, with antiserum to Dok-7 highlighted the accumulation of Dok-7 at neuromuscular junctions (Fig. 1, A to C), which are composed of the postsynaptic membrane with its densely clustered AChRs in close juxtaposition with the presynaptic nerve terminal. Therefore, we denervated a mouse gastrocnemius muscle by sciatic nerve resection to confirm the muscular, and thus postsynaptic, localization of Dok-7. One week after the operation, synaptophysin, a component of the presynaptic vesicle, was completely abolished in denervated muscles (fig. S4). However, the muscular localization of Dok-7 and AChRs remained intact, indicating a postsynaptic localization of Dok-7 at neuromuscular junctions (Fig. 1, D to F). Because postsynaptic differentiation and neuromuscular synapse formation are initiated at the endplate zone of skeletal muscle during embryogenesis (*9–11*), we performed a whole-mount in situ hybridization and found that Dok-7 transcripts are expressed in the central region encompassing the endplate area of the diaphragm muscles at day 14.5 of embryonic development (E14.5), when AChRs cluster in a nerve- and agrin-independent manner (fig. S5). Together, these results suggest that Dok-7 has the appropriate distribution to be involved in the neuromuscular junction.

Given the requirement for MuSK's PTB target motif and presumably its binding partner in postsynaptic specialization (*14*, *18*, *19*), we next examined the interaction of MuSK with Dok-7, which has a PTB domain, in 293T cells. These heterologous cells do not express either protein detectably, and forced expression of MuSK in these cells induced weak

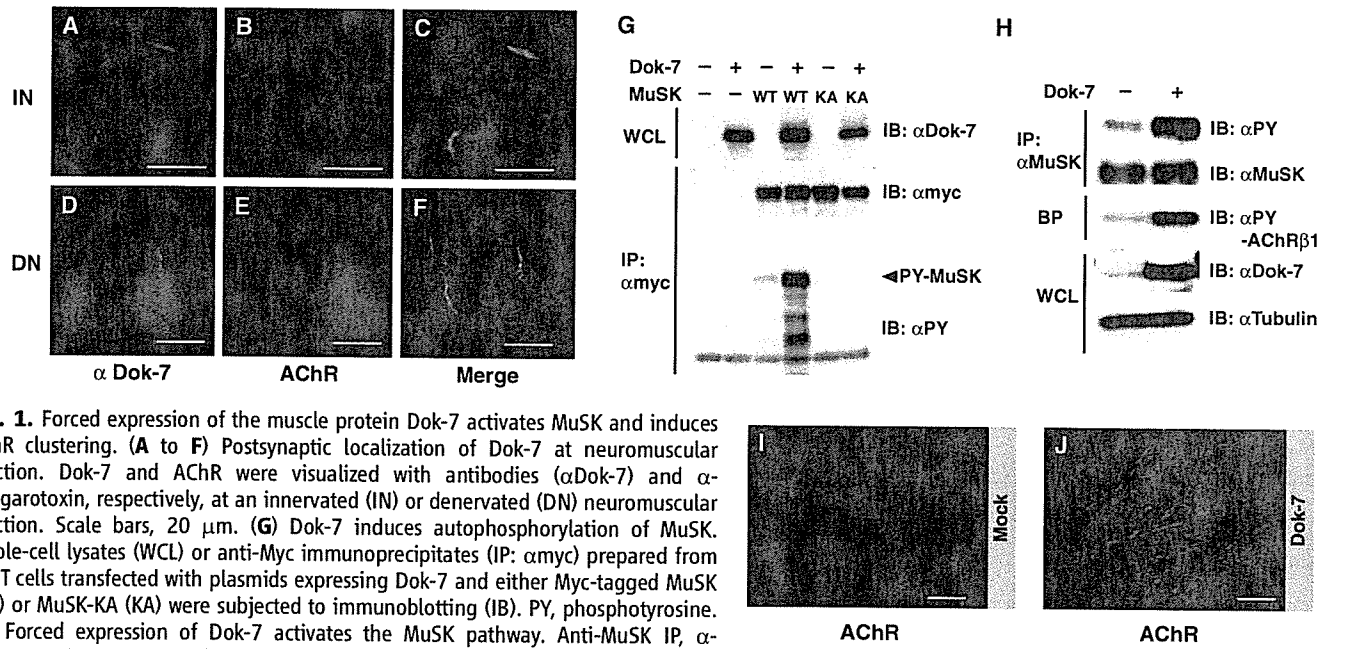

Fig. 1. Forced expression of the muscle protein Dok-7 activates MuSK and induces AChR clustering. (**A** to **F**) Postsynaptic localization of Dok-7 at neuromuscular junction. Dok-7 and AChR were visualized with antibodies (αDok-7) and α-bungarotoxin, respectively, at an innervated (IN) or denervated (DN) neuromuscular junction. Scale bars, 20 μm. (**G**) Dok-7 induces autophosphorylation of MuSK. Whole-cell lysates (WCL) or anti-Myc immunoprecipitates (IP: αmyc) prepared from 293T cells transfected with plasmids expressing Dok-7 and either Myc-tagged MuSK (WT) or MuSK-KA (KA) were subjected to immunoblotting (IB). PY, phosphotyrosine. (**H**) Forced expression of Dok-7 activates the MuSK pathway. Anti-MuSK IP, α-bungarotoxin precipitates (BP), or WCL from C2 myotubes transfected with plasmids for Dok-7 were subjected to IB. (**I** and **J**) Forced expression of Dok-7 induces aneural AChR clustering in C2 myotubes. Abundant clusters of AChRs formed in C2 myotubes transfected with Dok-7 expression plasmids (J), but only a few small clusters formed in the control (Mock) (I). Scale bars, 200 μm.

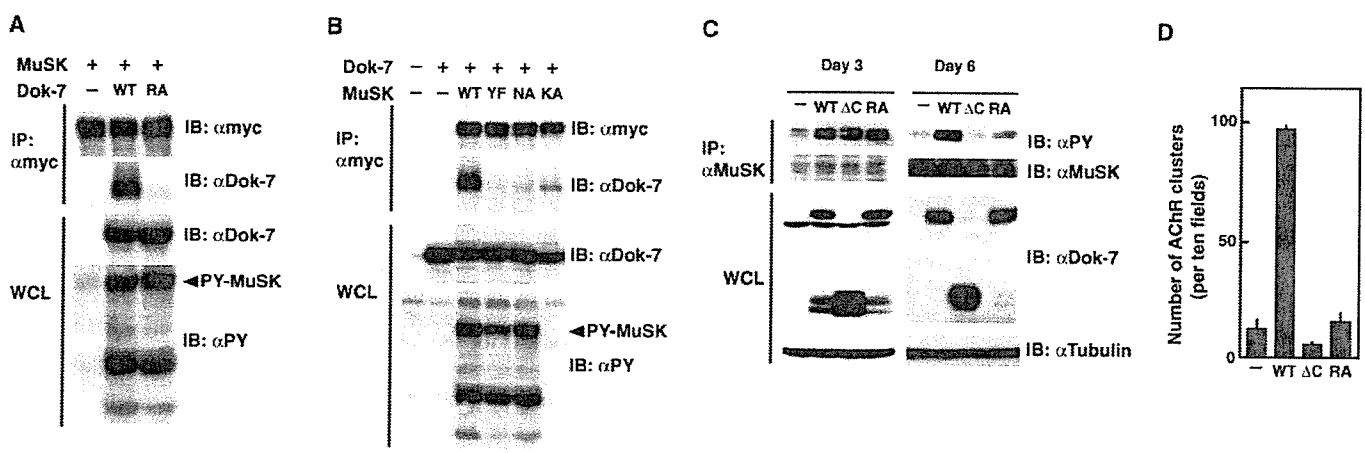

Fig. 2. Dok-7 interacts with MuSK by way of the PTB domain. (**A** and **B**) The PTB domain, its target, and kinase activity are essential for Dok-7 binding to MuSK. Anti-Myc IP or WCL from 293T cells transfected with plasmids for Dok-7 and Myc-tagged MuSK or their mutants, including MuSK-KA, were subjected to IB. (**C** and **D**) The PTB domain and C-terminal region are indispensable for the Dok-7–induced activation of MuSK and AChR clustering in fully differentiated C2 myotubes. Anti-MuSK IP or WCL from C2 cells transfected with expression plasmids for Dok-7 (WT), Dok-7–ΔC (ΔC), or Dok-7–RA (RA) were prepared at day 3 or 6 upon differentiation into myotubes and subjected to IB (C). The number of AChR clusters (mean ± SD) counted at day 7 is shown (D). Differentiation was achieved by day 6, whereas only a few myotubes had formed by day 3.